Global Change Biology

Global Change Biology (2017), doi: 10.1111/gcb.13566

Strong thermal acclimation of photosynthesis in tropical and temperate wet-forest tree species: the importance of altered Rubisco content

ANDREW P. SCAFARO[1,*], SHUANG XIANG[2,3,*], BENEDICT M. LONG[3,4], NUR H. A. BAHAR[1], LASANTHA K. WEERASINGHE[5], DANIELLE CREEK[6], JOHN R. EVANS[3,4], PETER B. REICH[6,7] and OWEN K. ATKIN[1]

[1]*ARC Centre of Excellence in Plant Energy Biology, Research School of Biology, The Australian National University, Building 134, Canberra, ACT 2601, Australia,* [2]*Chengdu Institute of Biology, Chinese Academy of Sciences, No. 9, Section 4, Renmin South Road, Chengdu Sichuan 610041, China,* [3]*Division of Plant Sciences, Research School of Biology, The Australian National University, Building 46, Canberra, ACT 2601, Australia,* [4]*ARC Centre of Excellence for Translational Photosynthesis, Research School of Biology, The Australian National University, Building 134, Canberra, ACT 2601, Australia,* [5]*Faculty of Agriculture, University of Peradeniya, 20400 Peradeniya, Sri Lanka,* [6]*Hawkesbury Institute for the Environment, Western Sydney University, Penrith, NSW 2751, Australia,* [7]*Department of Forest Resources, University of Minnesota, 1540 Cleveland Avenue North, St. Paul, MN 55108, USA*

Abstract

Understanding of the extent of acclimation of light-saturated net photosynthesis (A_n) to temperature (T), and associated underlying mechanisms, remains limited. This is a key knowledge gap given the importance of thermal acclimation for plant functioning, both under current and future higher temperatures, limiting the accuracy and realism of Earth system model (ESM) predictions. Given this, we analysed and modelled T-dependent changes in photosynthetic capacity in 10 wet-forest tree species: six from temperate forests and four from tropical forests. Temperate and tropical species were each acclimated to three daytime growth temperatures (T_{growth}): temperate – 15, 20 and 25 °C; tropical – 25, 30 and 35 °C. CO_2 response curves of A_n were used to model maximal rates of RuBP (ribulose-1,5-bisphosphate) carboxylation (V_{cmax}) and electron transport (J_{max}) at each treatment's respective T_{growth} and at a common measurement T (25 °C). SDS-PAGE gels were used to determine abundance of the CO_2-fixing enzyme, Rubisco. Leaf chlorophyll, nitrogen (N) and mass per unit leaf area (LMA) were also determined. For all species and T_{growth}, A_n at current atmospheric CO_2 partial pressure was Rubisco-limited. Across all species, LMA decreased with increasing T_{growth}. Similarly, area-based rates of V_{cmax} at a measurement T of 25 °C (V_{cmax}^{25}) linearly declined with increasing T_{growth}, linked to a concomitant decline in total leaf protein per unit leaf area and Rubisco as a percentage of leaf N. The decline in Rubisco constrained V_{cmax} and A_n for leaves developed at higher T_{growth} and resulted in poor predictions of photosynthesis by currently widely used models that do not account for T_{growth}-mediated changes in Rubisco abundance that underpin the thermal acclimation response of photosynthesis in wet-forest tree species. A new model is proposed that accounts for the effect of T_{growth}-mediated declines in V_{cmax}^{25} on A_n, complementing current photosynthetic thermal acclimation models that do not account for T sensitivity of V_{cmax}^{25}.

Keywords: climate modelling, earth system models, photosynthesis, photosynthesis modelling, Rubisco content, temperature, thermal acclimation, tropical trees, V_{cmax}

Received 26 June 2016 and accepted 16 October 2016

Introduction

Earth system models (ESMs) are used to predict current and future carbon fluxes between terrestrial ecosystems and the atmosphere (Arora *et al.*, 2013; Dufresne *et al.*, 2013). ESM land surface components rely heavily on understanding how environmental factors such as temperature (T) affect leaf-level carbon assimilation (Canadell *et al.*, 2007; Beer *et al.*, 2010). Given that global warming is leading to higher average daily temperatures in many biomes, how light-saturated rates of net photosynthetic CO_2 uptake (A_n) will respond to sustained changes in daytime growth temperature (T_{growth}) is a critical consideration for ESM predictions.

It has long been known that A_n often acclimates to sustained increases in T_{growth} (Berry & Bjorkman, 1980), via physiological, structural or biochemical adjustments that can contribute to increased optimum temperatures (T_{opt}) for A_n and/or altered photosynthetic capacity, when plants experience sustained higher T_{growth}

Correspondence: Owen K. Atkin, tel. +61 2 6125 5046, fax +61 2 6125 5095, e-mail: owen.atkin@anu.edu.au
*Denotes joint first author status.

(Lambers *et al*., 1998; Sage & Kubien, 2007; Smith & Dukes, 2013). Acclimation can result in rates of A_n being similar in cold and warm grown plants, when measured at prevailing T_{growth} of each treatment (i.e. homoeostasis). The degree of photosynthetic acclimation to temperature appears to be species and plant functional type (PFT) specific. For example, in a recent analysis of 70 studies (Way & Yamori, 2014), 76 of 150 species displayed increased T_{opt} and/or homoeostasis of A_n when they had acclimated to warmer T_{growth} conditions (termed constructive adjustment). In the remaining species, high T_{growth} was not associated with increased T_{opt} of A_n – in such cases, A_n at any given measuring T declines (termed detractive adjustment) in plants grown at higher T_{growth} (Way & Yamori, 2014). Interestingly, evergreen trees displayed constructive adjustments in only 36% of cases, less than C_3 herbs, C_4 plants or deciduous trees (Way & Yamori, 2014).

Notably, there are limited studies on photosynthesis acclimation for wet-forest tree species (Cunningham & Read, 2002, 2003; Cheesman & Winter, 2013). This is a problem for ESMs, as wet-forest trees – particularly those growing in the tropics – represent a major component of the global carbon cycle. Globally, biomass accumulation in tropical forests is estimated to have been 2369 Tg C yr^{-1} in recent years, compared with 574 Tg C yr^{-1} for boreal and temperate forests combined (Pan *et al*., 2011), highlighting the urgent need to understand how changes in T_{growth} affect photosynthesis of tropical species, including those growing in wet-forest ecosystems. Given the limited seasonal variations in T_{growth} in tropical regions (relative to the large seasonal variations in many temperate regions), some have speculated that wet-forest species from tropical equatorial regions may be less capable of acclimating than their temperate wet-forest counterparts (Cunningham & Read, 2003).

One powerful tool for understanding the mechanisms underpinning thermal acclimation of A_n is the widely used C_3 photosynthesis model of Farquhar *et al*. (1980). By measuring the response of A_n to changes in intercellular CO_2 partial pressure, the model allows for determination of when photosynthesis is ribulose-1,5-bisphosphate carboxylase/oxygenase (Rubisco) limited, or limited by the regeneration of the Rubisco substrate, ribulose-1,5-bisphosphate, termed A_c and A_r limited, respectively. The maximum velocity of CO_2 carboxylation (V_{cmax}) and the maximum photosynthetic electron transport capacity, driving RuBP regeneration, (J_{max}), are two important photosynthetic variables that can be calculated from the model. Triose phosphate utilization of photosynthetic product can be a third limitation on A_n capacity, but usually occurs at higher than physiologically relevant CO_2 partial pressures (Sharkey, 1985; Sharkey *et al*., 2007), although it can limit photosynthesis at low temperatures (Sage & Kubien, 2007) and when phosphate content at the site of photosynthesis is low (Ellsworth *et al*., 2015). Although at current atmospheric CO_2 partial pressures, light-saturated rates of A_n are predominantly A_c, A_r or colimited by both (Sage & Kubien, 2007), A_n is often A_c limited, especially at T_{opt}, particularly in trees (Hikosaka *et al*., 2006; Sage *et al*., 2008). Hence, V_{cmax} is often the critical component in determining photosynthetic capacity. V_{cmax} is determined by enzyme kinetics of Rubisco. Rubisco enzymatic activity at saturating substrate levels increases exponentially with T (von Caemmerer, 2000). Consequently, V_{cmax} exponentially increases with T until excess heat reduces the enzymatic capacity of Rubisco *in vivo* (Medlyn *et al*., 2002a; Hikosaka *et al*., 2006; Kattge & Knorr, 2007). The *in vivo* impairment of Rubisco activity at high T is unlikely to be due to impairment of Rubisco itself, which is heat stable to 45 °C and above (Crafts-Brandner & Salvucci, 2000; Sage, 2002; Yamori *et al*., 2006). Rather, inactive Rubisco at high T is often attributed to Rubisco activase (RCA), the heat-labile chaperone of Rubisco, responsible for keeping Rubisco active (Portis, 2003). It is well known that RCA is susceptible to high T and this susceptibility leads to a decline in carboxylation activity of Rubisco (Crafts-Brandner & Salvucci, 2000; Salvucci & Crafts-Brandner, 2004a; Sage *et al*., 2008). Importantly, synthesis of a heat-stable RCA is thought to be one of the main drivers of the acclimation process to increased T_{growth} (Sage & Kubien, 2007).

In situations where higher T_{growth} is not associated with a change in V_{cmax} at a common measurement T – usually taken as 25 °C (V_{cmax}^{25}) – then A_n is expected to increase with increasing T_{growth}, given the exponential T response of V_{cmax}, at least until RCA-mediated limitations start to play a role. Indeed, there are reports that indicate that V_{cmax}^{25} may not correlate strongly with T_{growth} (Kattge & Knorr, 2007; Way & Oren, 2010). V_{cmax}^{25} values do, however, differ among PFTs (Kattge *et al*., 2009; Ali *et al*., 2015). Moreover, there are reports that T_{growth}-dependent shifts in V_{cmax}^{25} occur in some species. For example, the arid shrub *Nerium oleander* L. (Badger *et al*., 1982), cool climate herbaceous spinach (*Spinacia oleracea*) (Yamori *et al*., 2005) and maritime pine, *Pinus pinaster Ait*. (Medlyn *et al*., 2002b), all show declines in V_{cmax}^{25} when growing at warmer T. In many cases, thermal acclimation also changes N partitioning between photosynthetic components and the ratio of J_{max} to V_{cmax} (when measured at 25 °C) which can lead to shifts in the A_n limitation dependent on T_{growth} (Hikosaka, 1997; Hikosaka *et al*., 1999; Onoda *et al*., 2005; Yamori *et al*., 2005, 2010; Kromdijk & Long, 2016). Given the possibility of common T_{growth}

adjustments to N partitioning and $V_{cmax}{}^{25}$, it is surprising that currently ESMs estimate V_{cmax} based on a simple assumed fixed relationship between V_{cmax} and N (Rogers, 2013).

The aim of our study was to determine how a wide range of T_{growth} values (15–35 °C) affect rates of light-saturated A_n and associated photosynthetic resource partitioning and capacity in 10 wet-forest tree species. We include both temperate (six) and tropical (four) species, beneficial in that modelling of wet-forest species photosynthesis in relation to temperature is underrepresented in the literature. We hypothesized: (1) that T_{growth} acclimation over a wide T-range will include adjustments to photosynthetic capacity; and (2), that underpinning the acclimation to higher T_{growth} are decreases in nitrogen partitioning to photosynthetic enzymes and resultant decreases in photosynthetic capacity. Species were grown 5 °C above and below their endemic mean maximum temperature by growing temperate species from 15 to 25 °C and tropical species from 25 to 35 °C. Therefore, comparison of acclimation properties between temperate and tropical individuals should not be confounded by one biome being exposed to temperatures further from that expected under *in situ* conditions. This is reasonable considering long-term (weeks to months) growth of a temperate species at 35 °C is as unrealistic of natural conditions as long-term growth of tropical species at 15 °C.

Materials and methods

Plant material and growth treatments

Six broad-leaf, evergreen, wet-forest temperate species from the southeast region of Australia (*Anoperus glandulosus*, *Atherosperma moschatum*, *Eucryphia lucida*, *Eucalyptus regnans*, *Hedycarya angustifolia*, *Tasmannia lanceolata*), and four broad-leaf, evergreen, wet-forest tropical species from the northeast region of Australia (*Castanopsermum australe*, *Cryptocarya mackinnoniana*, *Synima cordierorum*, *Syzygium sayeri*) were purchased from nurseries located in close proximity to each species' provenance (Table S1). The mean maximum temperature of the warmest month is 20.1 ± 0.8 °C for temperate and 30.0 ± 0.4 °C for tropical sites. Annual precipitation means for the two wet-forest biomes are similar and between 1700 and 1900 mm yr^{-1}. Plants were 30–45 cm in height upon arrival at the Australian National University (Canberra, ACT). Plants were re-potted into 2.8 L volume, free-draining pots, containing an organic potting mix, enriched with Osmocote® OSEX34 EXACT slow-release fertilizer with an N/P/K ratio of 16 : 3.9 : 10 (Scotts Australia, Bella Vista, NSW, Australia). Fertilizer was applied at a rate of 3 kg m^{-3} of potting mix, and re-applied after 2–3 months, ensuring luxury supply of nutrients throughout the experiment. Plants were watered daily to field capacity.

Re-potted plants were placed in temperature-controlled growth chambers (Thermoline, Wetherhill Park, Australia) located in the Research School of Biology 'Control Environment Growth Facility' at the ANU, Canberra, Australia. Plants were exposed to a constant photosynthetically active irradiance of 700–800 μmol photons m^{-2} s^{-1} and 70–80% relative humidity at [CO_2] of 400 μmol mol^{-1} (38.4 Pa, considering a mean atmospheric pressure of 96 kPa at the site of measurements) inside the growth chambers during the duration of the experiment. A 12 : 12-h dark : light photoperiod was maintained using 1000 Watt metal halide lamps (Multi-Vapor®; GE Lighting, Derrimut, Australia).

Before exposing plants to different T_{growth}, plants were grown in a T-controlled growth chamber for 1.5 months at 30/25 °C (day/night) for tropical species and at 20/15 °C for temperate species, approximating T_{growth} experienced by the selected tropical and temperate wet-forest species during the summer months (Xiang *et al*., 2013). The establishment period also enabled the seedlings to recover from transportation and transplanting shock. Plants were then either kept in the initial establishment T_{growth} or moved to matched growth cabinets (with relative humidity, CO_2 and growth irradiances identical to the initial condition) where the day/night growth T was 5 °C cooler or 5 °C warmer than the initial establishment condition. Consequently, tropical plants were exposed to day/night temperatures of 25/20 °C, 30/25 °C and 35/30 °C, and temperate plants were exposed to day/night regimes of 15/10 °C, 20/15 °C and 25/20 °C.

All experiments commenced 55 days after transferring to temperature treatments, on fully expanded leaves that developed during each temperature treatment. Temperate and tropical species were measured at T_{growth}, and at a common temperature of 25 °C by moving plants to the 25 °C growth cabinet prior to measurements. For all experiments, 3–5 biological replicates were sampled for each species, leading to a total of 114 individual analyses.

Gas-exchange measurements

All gas-exchange measurements were made using a Li-6400XT infrared gas-exchange analyser (LICOR, Lincoln, NE, USA). Intercellular CO_2 (C_i) dependence of net assimilation (A_n) was determined by generating A_n-C_i curves by adjusting Li-6400XT reference chamber CO_2 partial pressures, in the following chronological order: 38.4, 28.8, 19.2, 14.4, 12.0, 9.6, 7.2, 4.8, 2.4, 38.4, 57.6, 86.4, 120, 144, 163.2 and 192 Pa. Ten measurements were logged for each set point after photosynthesis stabilization, and all measurements included when generating A_n-C_i curves. Photosynthetically active radiation (PAR) was set to 1800 μmol photons m^{-2} s^{-1} and a flow rate of 500 μmol s^{-1} set for all A-C_i measurements. At the completion of the final CO_2 measurement, reference CO_2 was returned to 38.4 Pa and the leaf within the cuvette was dark adapted for 30 min before a final 10 measurements were logged for capturing dark respiration rates (R_{dark}). The Licor 'block' T was set to the glasshouse temperature, and the mean leaf T for every A_n-C_i curve was within ±1.3 °C of ambient air. The vapour pressure deficit based on leaf temperature ranged

from 1 to 3.2 kPa across all measurement temperatures and relative humidity ranged from 46% to 66%. Subsequent to gas-exchange measurements, gasket CO_2 diffusion was corrected for, as previously described (Bruhn *et al*., 2002).

Photosynthesis modelling

A_n-C_i were converted to A_n-C_c curves, with partial pressure (Pa) of CO_2 at the site of the chloroplast (C_c), calculated from

$$C_c = C_i - \frac{A_n}{g_m}, \quad (1)$$

where g_m (μmol m^{-2} s^{-1} Pa^{-1}) is the mesophyll conductance. g_m at 25 °C was set to 3.1 μmol m^{-2} s^{-1} Pa^{-1} for all species, calculated from the average of two temperate tree species (*Eucalyptus pauciflora* and *Quercus engelmannii*), and one tropical species (*Lophostemon confertus*), measured using carbon isotope discrimination (von Caemmerer & Evans, 2015). g_m was adjusted to measurement temperature using the equation:

$$g_m = \frac{1}{\frac{1}{g_{liq}} + \frac{1}{g_{mem}}}, \quad (2)$$

where g_{liq} is conductance through the liquid phase (0.36 μmol s^{-1} at 25 °C) and g_{mem} is conductance through the membrane phase (0.0484 μmol s^{-1} at 25 °C), and the energy of activation (61.7 kJ mol^{-1}) determining the temperature response of g_{mem} was taken as the average values of the three aforementioned species [refer to von Caemmerer & Evans (2015) for comprehensive details].

Photosynthesis was modelled using the C_3 photosynthesis model of Farquhar *et al*. (1980), assuming either Rubisco (A_c) or RuBP regeneration (A_r) limitation. A_c limited photosynthesis was modelled using the equation

$$A_c = \frac{V_{cmax}(C_c - \Gamma^*)}{C_c + K_c\left(1 + \frac{O}{K_o}\right)} - R_{light}, \quad (3)$$

where V_{cmax} (μmol m^{-2} s^{-1}) is the maximum rate of RuBP carboxylation, K_c (27.24 Pa) and K_o (16.58 kPa) are the Rubisco Michaelis constants for CO_2 and O_2, respectively, O (21 kPa) is the O_2 partial pressure, R_{light} is the light respiration, and Γ* is the CO_2 compensation point in the absence of respiration (3.74 Pa). Γ*, K_c and K_o and their scaling constants (*c*) of 13.49, 38.28 and 14.68, respectively, and the energy of activation (E_a) of 24.46, 80.99 and 23.72, respectively, was taken from tobacco (Bernacchi *et al*., 2002). V_{cmax} and R_{light} were initially set to *y*-axis maximum and the value of *y* at *x*-axis minimum, respectively, and were solved by iteration, using a nonlinear least-squares fit, using the graph and statistical software GRAPHPAD PRISM 5.0d (GraphPad Prism Software, Inc., San Diego, CA, USA). Through visual inspection, the A_c curve was fit only to A_n measurements below a C_c value which corresponded with Rubisco limitation. Where the transition point was ambiguous, reducing the sum of squares of the modelled curve refined the points fitted. RuBP-limited photosynthesis (A_r) was modelled using the equation:

$$A_r = \frac{J_{max}(C_c - \Gamma^*)}{4C_c + 8\Gamma^*} - R_{light}, \quad (4)$$

where J_{max} is the maximum rate of chloroplast electron transport. For A_r, R_{light} was taken as the value solved using A_c modelling. J_{max} was solved by iteration, for A_n measurements above a C_c value, as explained above.

Temperature response functions

The temperature response of V_{cmax} and J_{max} was modelled in two commonly reported ways, differing in that one is generated from a single T_{growth}, while the other incorporates thermal acclimation adjustments in V_{cmax} and J_{max} to sustained differences in T_{growth}. The first method, not incorporating acclimation, was using the standard Arrhenius function:

$$V_{cmax}{}^{25}\exp^{\left(\frac{c - E_a}{\mathcal{R}T_l}\right)}, \quad (5)$$

with the parameter being either V_{cmax} or J_{max} measured at 25 °C. *c* is the scaling constant, and E_a is the energy of activation (both presented in kJ mol^{-1}). For V_{cmax}, *c* and E_a were set to 26.36 and 65.33, respectively, and for J_{max}, *c* and E_a were set to 17.71 and 43.9, respectively, obtained from *in vivo* measurements of tobacco grown at 25 °C (Bernacchi *et al*., 2002). Alternatively, for V_{cmax}, *c* and E_a were solved by iteration in the same manner as A_c and A_r mentioned above. $\mathcal{R}$ is the molar gas constant (8.314 J mol^{-1} K^{-1}), and T_l is the temperature of the leaf in Kelvin (K).

The second method used a peaked model, with refinement to account for acclimation driven changes in the *T*-optimum of V_{cmax} or J_{max} by Kattge & Knorr (2007), with V_{cmax} and J_{max} calculated as:

$$V_{cmax} = V_{cmax}{}^{25}\exp^{\frac{H_a(T_l - T_{ref})}{T_{ref}\mathcal{R}T_l}}\frac{1 + \exp\left(\frac{T_{ref}\left(a_{\Delta S,V} + b_{\Delta S,V} * T_{growth}\right) - H_d}{T_{ref}\mathcal{R}}\right)}{1 + \exp\left(\frac{T_l\left(a_{\Delta S,V} + b_{\Delta S,V} * T_{growth}\right) - H_d}{T_l\mathcal{R}}\right)}, \quad (6)$$

and,

$$J_{max} = \left(a_{rJ,V} + b_{rJ,V} * T_{growth}\right)V_{cmax}{}^{25}\exp^{\frac{H_a(T_l - T_{ref})}{T_{ref}\mathcal{R}T_l}}\frac{1 + \exp\left(\frac{T_{ref}\left(a_{\Delta S,J} + b_{\Delta S,J} * T_{growth}\right) - H_d}{T_{ref}\mathcal{R}}\right)}{1 + \exp\left(\frac{T_l\left(a_{\Delta S,J} + b_{\Delta S,J} * T_{growth}\right) - H_d}{T_l\mathcal{R}}\right)}, \quad (7)$$

where $V_{cmax}{}^{25}$ is the base rate of V_{cmax} at a measured temperature of 25 °C. T_l is the leaf temperature and T_{ref} is the reference temperature (i.e. 25 °C), both expressed in Kelvin. The enthalpy (H_a) was set at 71.5 kJ mol^{-1} for V_{cmax} and 50 kJ mol^{-1} for J_{max}. H_d is the deactivation enthalpy and was set at 200 kJ mol^{-1} for both V_{cmax} and J_{max}. The term ($a_{\Delta S}$+$b_{\Delta S}$*T_{growth}) is the entropy factor (Δ*S*) adjusted for the growth temperature (T_{growth} in °C), by taking into account the intercept (*a*) and slope (*b*) of a linear regression analysis between Δ*S* and T_{growth} for V_{cmax} (0.6684 kJ mol^{-1} and −1.07 kJ mol^{-1} $°C^{-1}$ for *a* and *b*, respectively) or J_{max} (0.6597 kJ mol^{-1} and −0.75 kJ mol^{-1} $°C^{-1}$ for *a* and *b*,

respectively). For the nonacclimated model of V_{cmax} and J_{max}, ΔS was set at 0.649 kJ mol^{-1} and 0.646 kJ mol^{-1} °C^{-1}, respectively. All parameters, except for the term described below, were taken from Kattge & Knorr (2007).

To adjust J_{max} to the base rate of $V_{cmax}{}^{25}$, the intercept and slope of the fraction of J_{max} to V_{cmax} at 25 °C was accounted for through the term $a_{rJ,V} + b_{rJ,V} * T_{growth}$, with the intercept and slope set to 2.9 and −0.032, respectively, derived from the J_{max} to V_{cmax} values at 25 °C ($J_{max}{}^{25}/V_{cmax}{}^{25}$), obtained in this study (Table 1), rather than the $J_{max}{}^{25}/V_{cmax}{}^{25}$ presented by Kattge & Knorr (2007).

Leaf mass, area, nitrogen, chlorophyll and Rubisco quantification

Leaves were collected following gas-exchange measurements. Initially, the fresh mass of leaf material used in the gas-exchange measurements was determined (Mettler-Toledo Ltd, Port Melbourne, Vic, Australia); thereafter, leaf area was measured using a LI-3100 leaf area meter (Li-COR, Inc. Lincoln, NE, USA). Gas-exchange leaves were oven dried at 70 °C for >48-h, weighed and leaf dry mass per unit leaf area (LMA) calculated. Total N of dried leaves was calculated using the Kjeldahl acid digest method (Allen *et al.*, 1974). Additional measurements (i.e. chlorophyll and protein abundance) were also made on leaf discs taken from the closest, adjacent fully expanded leaf to that used in the gas-exchange measurements. Chlorophyll content of two 0.77 cm^2 snap-frozen leaf discs was extracted by grinding in a mortar and pestle, in acetone with 2.5 mM $MgCO_3$. The supernatant absorbance was read on a UV–VIS spectrometer (Lambda 25; Perkin Elmer, Shelton, CT, USA). Rubisco content was measured by homogenizing leaf discs into powder using a Qiagen Tissue-Lyzer 48 (Qiagen, Venlo, the Netherlands). Due to high phenolic content and rapid oxidation of samples during extraction, the application required a specific extraction procedure in order to allow the determination of Rubisco content. Protein was extracted from tissue powder using extraction buffer, following the method of Gaspar *et al.* (1997), as adapted by Bahar *et al.* (2016), with all procedures undertaken on ice. 4× SDS-PAGE sample buffer (Invitrogen, Carlsbad, CA, USA) was added to soluble protein and loaded in equal volumes on 4–12% NuPage Bis-Tris polyacrylamide gels (Invitrogen). Rubisco purified from *N. tabacum* (tobacco) was loaded onto gels in varying concentrations to generate a standard curve of Rubisco large subunit (LSU) quantities. The quantity of tobacco Rubisco used as a standard was predetermined using radiolabelled [^{14}C]carboxypentitol-P_2 (Ruuska *et al.*, 1998). Gels were stained with GelCode Blue stain reagent (ThermoFisher Scientific, Scoresby, Vic, Australia), and image analysis of protein bands using a Versa-Doc (Bio-Rad, Hercules, CA, USA) provided quantification of Rubisco, by comparing purified standards with the corresponding Rubisco bands of each sample (Fig. S1).

Statistical analysis

Leaf trait means and standard deviations for each temperate and tropical species at each measured temperature are provided (Tables S2 and S3). We performed linear regression analysis of leaf traits as a function of T_{growth} for all species means. Temperate and tropical species data sets were treated separately and as one. If there was no difference in slopes or intercepts for the two data sets, as determined by an ANOVA of the slope and intercept means (Table 1), then linear regression analysis across the entire temperature range, irrespective of biome, was explored. For the temperature response curve analysis of V_{cmax} and J_{max}, the nonlinear goodness of fit (R^2) is based on the mean value of all species combined at each T_{growth}. All graphs, statistical analysis and model fits were achieved through the graph, statistical and curve fitting software GRAPHPAD PRISM 5.0d.

Results

Growth temperature adjustments in leaf anatomical and chemical properties

For many leaf traits, we found similar T_{growth} responses among species. For example, in most temperate and tropical wet-forest species, area-based Rubisco content and $V_{cmax}{}^{25}$ decreased with increasing T_{growth} (Fig. S2). Given the general similarity in trait temperature responses in temperate and tropical species, we chose to show at each T_{growth} trait values averaged across all species within each biome group (e.g. Figs 1, 3 and 6), with regression analyses and ANOVAs (Table 1) being used to test whether there were significant differences in the slope and/or intercept of trait–T_{growth} relationships between the two biome groups; for these analyses, analyses were carried out using species mean values, but with the figures showing biome-group means. For most traits, there was no significant difference in the slopes and/or intercept means between the two biome groups (Table 1). Given this, one can fit a common regression across both biomes when plotting trait values against T_{growth} for those traits with significant T_{growth}-dependent changes in trait values. An example is the decline in area-based Rubisco content ($Rubisco_a$) with increasing T_{growth} (Fig. 1a). Although LMA also decreased with increasing T_{growth} (Fig. 1b), the fall in $Rubisco_a$ was not due to this LMA decline alone, as there was an associated increase in N on a dry mass basis (N_m) with increasing T_{growth} (Fig. 1c), counteracting the reduction in LMA and leading to no significant decline in nitrogen on an area basis (N_a; Fig. 1d). The decline in $Rubisco_a$ was therefore not due to any T_{growth}-dependent change in N_a but rather a reduced allocation of N content to Rubisco, evident in Rubisco as a percentage of leaf N declining with increasing T_{growth} (Fig. 1e). Of note, no significant T_{growth}-dependent decrease in Rubisco on a dry mass basis was observed (Fig. 1f), as the decline in Rubisco as a percentage of N was counteracted by the increase in N_m with increasing T_{growth}.

Table 1 Linear regression analysis and ANOVA of leaf trait (*y*-value) responses to daytime growth temperature (*x*-value), for temperate, tropical and both temperate and tropical species combined

	Temperate				Tropical				Slope Comparison		Intercept Comparison		Combined			
Leaf trait	Slope	Intercept	r^2	P	Slope	Intercept	r^2	P	F	P	F	P	Slope	Intercept	r^2	P
LMA	−2.09 ± 1.68	137 ± 34	0.09	0.230	−0.783 ± 0.704	92.4 ± 21.3	0.11	0.292	0.37	0.549	0.63	0.435	−2.20 ± 0.663	138 ± 16.5	0.28	0.003*
N_m	0.185 ± 0.203	18.9 ± 4.2	0.05	0.377	0.42 ± 0.42	14.7 ± 12.7	0.09	0.339	0.32	0.577	0.56	0.461	0.397 ± 0.129	15.0 ± 3.2	0.25	0.005*
N_a	−0.023 ± 0.032	2.56 ± 0.644	0.03	0.471	0.011 ± 0.022	1.51 ± 0.65	0.02	0.632	0.63	0.435	0.38	0.541	−0.020 ± 0.013	2.46 ± 0.33	0.07	0.147
$Rubisco_{\%\ N}$	−0.370 ± 0.160	14.4 ± 3.3	0.25	0.034	−0.196 ± 0.172	11.8 ± 5.2	0.12	0.280	0.52	0.479	1.5	0.238	−0.192 ± 0.076	11.2 ± 1.9	0.19	0.017*
$Rubisco_a$	−0.763 ± 0.285	28.4 ± 5.8	0.31	0.016	−0.221 ± 0.261	16.2 ± 7.9	0.07	0.416	1.7	0.197	0.48	0.493	−0.438 ± 0.129	22.2 ± 3.2	0.29	0.002*
$Rubisco_m$	−0.006 ± 0.003	0.27 ± 0.07	0.18	0.072	−0.003 ± 0.005	0.22 ± 0.16	0.02	0.628	0.43	0.516	1.66	0.210	−0.002 ± 0.002	0.19 ± 0.05	0.04	0.266
A_a	−0.188 ± 0.195	13.6 ± 4.0	0.05	0.350	−0.101 ± 0.124	9.7 ± 3.8	0.06	0.433	0.11	0.744	0.98	0.331	−0.249 ± 0.081	14.5 ± 2.0	0.25	0.005*
A_m	−0.272 ± 2.48	115 ± 51	<0.00	0.914	−0.271 ± 2.60	109 ± 79	<0.00	0.919	<0.00	1	0.05	0.819	−0.589 ± 1.12	120 ± 28	0.01	0.604
g_s	−0.002 ± 0.005	0.18 ± 0.10	0.01	0.688	−0.002 ± 0.003	0.17 ± 0.08	0.07	0.413	<0.00	0.977	0.21	0.654	−0.003 ± 0.002	0.20 ± 0.05	0.09	0.116
C_i	0.046 ± 0.11	25.4 ± 2.3	0.01	0.694	−0.120 ± 0.21	28.6 ± 6.4	0.03	0.582	0.57	0.460	0.68	0.418	−0.088 ± 0.068	27.9 ± 1.7	0.06	0.205
C_c	0.193 ± 0.13	19.0 ± 2.7	0.01	0.170	−0.0319 ± 0.22	24.2 ± 6.8	<0.00	0.865	0.9	0.352	0.24	0.628	0.0550 ± 0.076	21.6 ± 1.9	0.02	0.473
R_{light}	−0.037 ± 0.047	3.6 ± 1.0	0.04	0.437	0.020 ± 0.017	0.71 ± 0.51	0.12	0.273	0.91	0.349	14	0.001*	−0.097 ± 0.022	4.6 ± 0.6	0.40	<0.001*
R_{dark}	0.013 ± 0.018	1.1 ± 0.4	0.03	0.466	0.016 ± 0.026	0.8 ± 0.8	0.04	0.548	0.01	0.917	1.9	0.182	−0.001 ± 0.009	1.4 ± 0.2	<0.00	0.923
R_{dark}/V_{cmax}	−0.002 ± 0.001	0.075 ± 0.023	0.15	0.116	−0.002 ± 0.001	0.081 ± 0.017	0.49	0.011	<0.00	0.959	0.64	0.429	−0.0014 ± 0.0004	0.067 ± 0.011	0.26	0.004*
V_{cmax}^{25}	−1.13 ± 0.94	80 ± 19	0.08	0.250	−0.381 ± 0.843	48 ± 26	0.02	0.661	0.30	0.586	2.2	0.148	−1.57 ± 0.43	86 ± 11	0.33	0.001*
$V_{cmax}^{25}{}_{,\ N}$	−0.67 ± 0.74	44 ± 15	0.05	0.378	−0.332 ± 0.521	30 ± 16	0.04	0.539	0.11	0.738	0.67	0.419	−0.644 ± 0.278	40 ± 7	0.16	0.028*
J_{max}^{25}	−1.7 ± 2.1	165 ± 43	0.04	0.441	−1.2 ± 1.3	98 ± 39	0.08	0.373	0.03	0.873	9.8	0.004*	−4.7 ± 0.9	218 ± 25	0.45	<0.001*
$J_{max}^{25}/V_{cmax}^{25}$	0.021 ± 0.020	1.9 ± 0.4	0.07	0.298	−0.022 ± 0.014	2.5 ± 0.4	0.20	0.145	2.6	0.118	12	0.002*	−0.032 ± 0.010	2.9 ± 0.2	0.26	0.004*

The regression analysis is based on the plots of mean leaf trait values for each species against corresponding growth temperature. The leaf traits are dry leaf mass per area, LMA ($g_{DM}\ m^{-2}$); N on a dry mass basis, N_m (mg g_{DM}^{-1}); N on an area basis, N_a(g m^{-2}); Rubisco as a % of N, $Rubisco_{\%N}$; Rubisco on an area basis, $Rubisco_a$ (μmol sites m^{-2}); Rubisco on a dry mass basis, $Rubisco_m$ (μmol sites g_{DM}^{-1}); net assimilation on an area basis, A_a (μmol CO_2 m^{-2} s^{-1}); net assimilation on a dry mass basis, A_m (μmol CO_2 g_{DM}^{-1} s^{-1}); stomatal conductance, g_s (mol m^{-2} s^{-1}); intercellular CO_2 partial pressure, C_i (Pa); chloroplast CO_2 partial pressure, C_c (Pa); respiration in the light, R_{light} (μmol CO_2 m^{-2} s^{-1}); respiration in the dark, R_{dark} (μmol CO_2 m^{-2} s^{-1}); R_{dark} as a fraction of maximum CO_2 carboxylation velocity, R_{dark}/V_{cmax}; V_{cmax} measured at a common 25 °C, V_{cmax}^{25} (μmol CO_2 m^{-2} s^{-1}); V_{cmax}^{25} as a fraction of N, $V_{cmax}^{25}{}_{,\ N}$ (μmol CO_2 m^{-2} s^{-1} g N^{-1}); maximum photosynthetic electron transport capacity measured at a common 25 °C, J_{max}^{25} (μmol e^- m^{-2} s^{-1}); J_{max}^{25} as a fraction of V_{cmax}^{25}, $J_{max}^{25}/V_{cmax}^{25}$. Temperate and tropical species were initially analysed separate from one another, followed by a comparison of slopes and intercepts. If the slopes between separate temperate and tropical species analysis were not significantly different (slope comparison), all measurements, irrespective of biome, were pooled (combined analysis). Slope and intercept values are means ± standard errors. Explained variance (r^2) and probability values (P) are given, as well as F-test scores (F) for slope and intercept comparisons. The degrees of freedom for temperate, tropical and combined analysis were 16, 10 and 28 for all.

*Indicates significant differences ($P < 0.05$) in the comparison and combined analysis.

 Global Change Biology, doi: 10.1111/gcb.13566

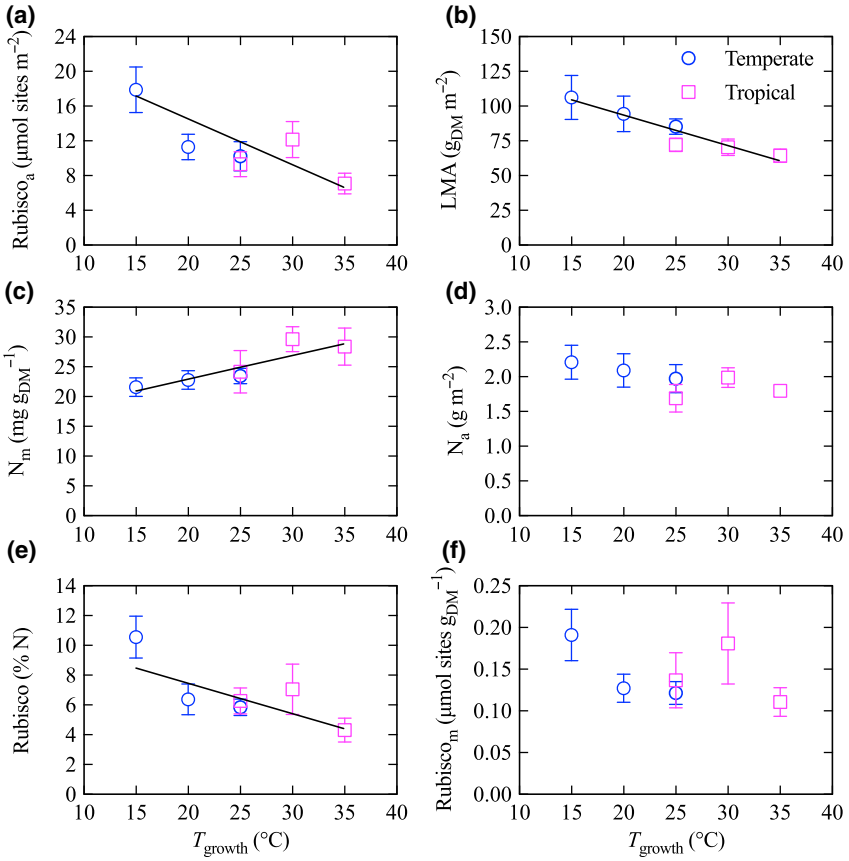

Fig. 1 Leaf properties for six temperate and four tropical tree species grown and measured from 15 to 35 °C. The number of Rubisco active sites on an area basis (a), leaf mass per area (LMA) (b), leaf N on a mass (c) and area basis (d), Rubisco as a percentage of N (e), and on a mass basis (f) are presented. Solid black lines indicate significant ($P < 0.05$) linear regression of combined temperate and tropical values, for all individual species means, over the entire temperate range (refer to Table 1 for regression analysis). Open blue circles indicate measurements of temperate species and open magenta squares indicate tropical species. Values are the mean ± standard error of the species means at each measured temperature.

Photosynthetic acclimation to growth temperature

The manner in which Rubisco (A_c) and RuBP regeneration (A_r) limitations regulate light-saturated rates of net photosynthesis (A_n) with increasing C_c is presented in Fig. 2. Results are shown separately for temperate and tropical trees (averaged across species), grown in the range of 15–35 °C. Individual species A_n-C_c responses are shown in Fig. S3. A_c models provided a high degree of accuracy ($R^2 = 0.98 \pm 0.02$) in estimating the measured data. In general, temperate species became A_r limited at higher C_c than their tropical counterparts, although variation in transitions from A_c to A_r limitation is noted between species within each biome (Fig. S3). Even so, irrespective of T_{growth} or biome-origin, A_n at the current ambient CO_2 partial pressure (C_a) of 38.4 Pa, and both saturating light of 1800 μmol photons m^{-2} s^{-1} and without water limitations, was in all cases, Rubisco-limited (Fig. 2). Indeed, all biological replicates for all species were A_c limited at a C_a of 38.4 Pa (Fig. S3). In most cases, A_n did not become A_r limited until C_c partial pressure was >40 Pa, equivalent to a C_a of about 57.6 Pa, well above current C_a. A_r models did not fit the observations as well ($r = 0.67 \pm 0.18$), perhaps reflecting J_{max} not being reached within the C_c range measured in all species (Fig. S3).

There was a significant negative linear relationship between light-saturated net assimilation (at current C_a of 38.4 Pa) on an area basis (A_a) and T_{growth}, when temperate and tropical species were combined (Fig. 3a, Table 1). The adjustment of A_a was considerable, averaging ≈2.5 μmol m^{-2} s^{-1} for every 10 °C shift in T_{growth}. Area-based leaf stomatal conductance (g_s) followed a similar pattern as for A_a, with the g_s–T_{growth} relationship being significant at $P = 0.11$. Rates of net assimilation on a mass basis (A_m; again measured at T_{growth}) did not significantly vary with T_{growth}, indicating homoeostasis of mass-based carbon gain across the

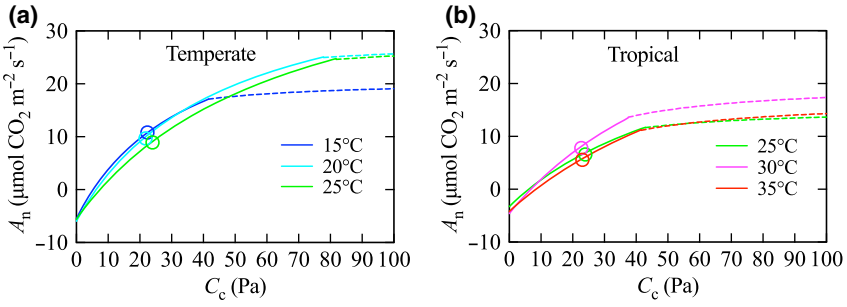

Fig. 2 The modelled response of net assimilation (A_n) to changes in chloroplast CO_2 partial pressure (C_c) for six temperate tree species grown at 15, 20 and 25 °C (a), and four tropical tree species grown at 25, 30 and 35 °C (b). Solid lines indicate Rubisco limitation (A_c), and dashed lines indicate RuBP regeneration limitation (A_r). Open circles are A_n values when ambient CO_2 was equal to 38.4 Pa. Each curve is the mean of 20, 20, 22, 19, 16 and 16 individually modelled A_n-C_c data sets for temperate species at 15, 20 and 25 °C and tropical species at 25, 30 and 35 °C, respectively. Photosynthesis was modelled using the published Rubisco kinetic parameters of tobacco grown at 25 °C, as presented by Bernacchi *et al.* (2002).

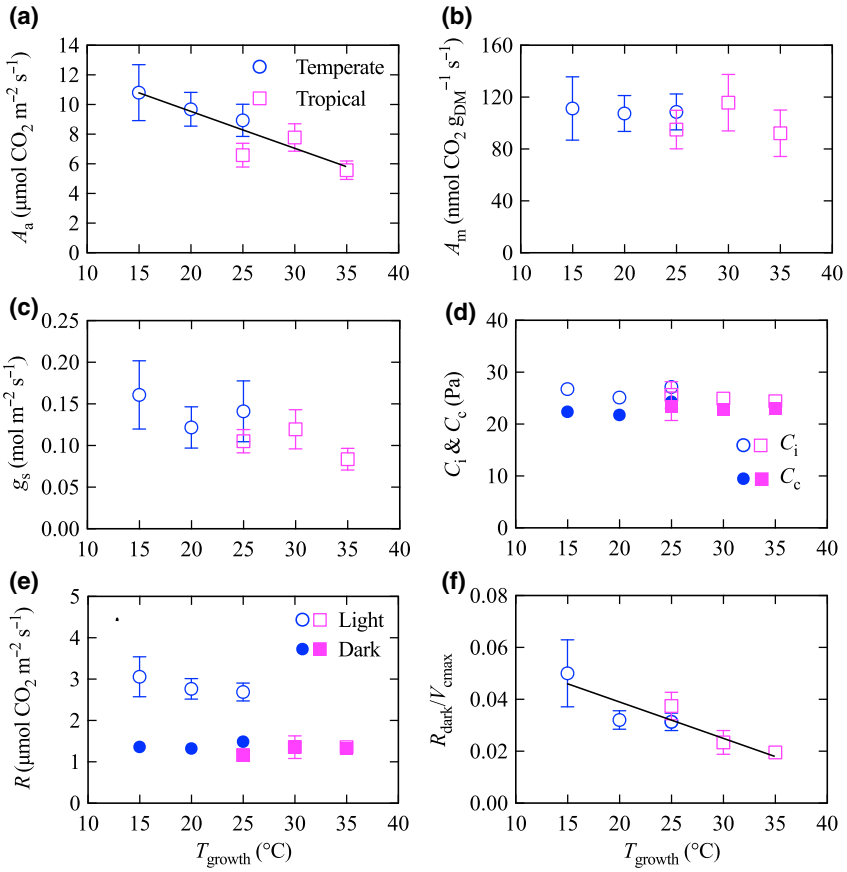

Fig. 3 Net assimilation (A_n), stomatal conductance (g_s), internal CO_2 partial pressures (C_i and C_c) and respiration (R_{light} and R_{dark}) of temperate (blue circles) and tropical (magenta squares) tree species across the daytime growth temperature range of 15–35 °C (T_{growth}), at an ambient CO_2 partial pressure of 38.4 Pa. (a, b, c) Net assimilation, on an area (A_a) and dry mass basis (A_m), and stomatal conductance (g_s). (d) Intercellular CO_2 (C_i – open symbols) and chloroplast CO_2 (C_c – closed symbols). (e) R_{light}, extrapolated from A_n–C_c modelling (open symbols), as well as R_{dark} (closed symbols) from direct gas-exchange measurements. Note that rates of R_{light} of the tropical species were near identical to those in darkness, and symbols are thus not visible. (f) R_{dark} as a fraction of V_{cmax}. Solid black lines indicate significant ($P < 0.05$) linear regression of individual species means when temperate and tropical data sets were combined (refer to Table 1). Values are the mean ± standard error of the species means at each growth temperature.

20 °C range of T_{growth} values. Intercellular CO_2 partial pressure (C_i) was stable over the entire temperature range, as was calculated chloroplast CO_2 partial pressure (C_c) and the difference between the two never exceeded 4.3 Pa (Fig. 3d). Temperate species exhibited higher estimated R_{light} than tropical species (Fig. 3e; note that rates of R_{light} of the tropical species were near identical to those in darkness, and symbols are thus not visible), as seen by the significant difference in the y-intercept of regression analysis between the two biomes (Table 1). R_{light} did not show a significant linear decline with increased T_{growth} for each biome analysed individually (Fig. 3e, Table 1). Respiration in the dark (R_{dark}), measured directly from gas-exchange measurements in darkness at T_{growth}, was stable across the entire T_{growth} range and values for temperate and tropical biomes were similar (Fig. 3e), indicating very strong thermal acclimation. Due to the temperature stability of respiration (i.e. homoeostasis) but not of V_{cmax}, R_{dark} as a fraction of photosynthetic capacity (R_{dark}/V_{cmax}) significantly declined in response to increasing temperature (Fig. 3f).

T_{growth} implications on the short-term temperature dependence of V_{cmax}

We assessed how acclimation to a wide range of T_{growth} impacted on the immediate temperature response of V_{cmax}. To achieve this, the V_{cmax} of each species and T_{growth} was measured shortly after moving plants to a common 25 °C ($V_{cmax}{}^{25}$). By plotting V_{cmax} measured at each respective T_{growth}, as a fraction of V_{cmax} measured at 25 °C ($V_{cmax}{}^{g/25}$), an immediate temperature response curve of V_{cmax} was generated (Fig. 4a). In doing so, we could assess the impact of short-term changes in measuring T on V_{cmax} values for cool and warm acclimated plants. The solid curves in Fig. 4a follow the standard Arrhenius function, with an exponential increase in V_{cmax} with rising temperature [red curve – derived from tobacco grown at 25 °C (Bernacchi *et al.*, 2002); black curve – iteratively fit]. Interestingly, the Arrhenius functions provided excellent fits to the observed $V_{cmax}{}^{g/25}$ values of both temperate and tropical trees [R^2 = 0.97 for Bernacchi *et al.* (2002) or R^2 = 0.99 by iteration; Table 2], despite the modelled V_{cmax} temperature response curve of Bernacchi *et al.* (2002) being derived from tobacco, grown only at 25 °C, a powerful indication that Rubisco enzymatic properties, independent of activation state, do not significantly adjust to T_{growth}.

Next, we used the peaked model of Kattge & Knorr (2007), which accounts for declines in V_{cmax} at above optimal T. The peaked model parameterized to each measured T_{growth} fit closely with the corresponding

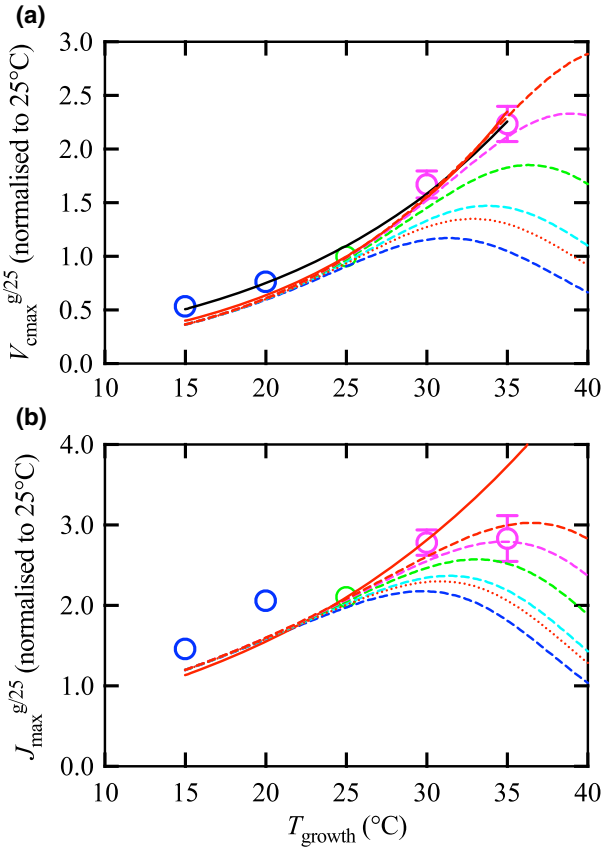

Fig. 4 The immediate temperature response of maximum CO_2 carboxylation rates (V_{cmax}) (a) and photosynthetic electron transport rates (J_{max}) (b), acclimated to daytime growth temperatures (T_{growth}) from 15 to 35 °C (open circles). (a) V_{cmax} at T_{growth} was expressed as a fraction of V_{cmax} measured but not grown at 25 °C ($V_{cmax}{}^{g/25}$) and normalized to a value of 1 at 25 °C. (b) Similarly, J_{max} at, T_{growth} as a fraction of J_{max} measured but not grown at 25 °C ($J_{max}{}^{g/25}$) and normalized to a value of 1 at 25 °C. Solid red curves and solid black curves are the Arrhenius temperature response function of V_{cmax} and J_{max}, parameterized for tobacco (Bernacchi *et al.*, 2002), or solved by iteration to the measured values, respectively. Dashed blue, cyan, green, magenta and red curves are the peaked model temperature response function of V_{cmax} and J_{max}, acclimated to 15, 20, 25, 30 and 35 °C, respectively (Kattge & Knorr, 2007). The red dotted curves are the nonacclimated peaked model function. Values are the mean ± standard error of the species means at each measured temperature.

V_{cmax} measurement, as well as all measurements below the set acclimation temperature. Thus, the peaked model, with the entropy factor (ΔS) adjusted to a T_{growth} of 35 °C, was a good fit (R^2 = 0.97) to the entire range of V_{cmax} from 15 to 35 °C (Fig. 4a, Table 2). However, the peaked model without acclimation (i.e. no T_{growth} adjustments in ΔS) resulted in reduced accuracy (R^2 = 0.47), supporting the need for an acclimation term in the peaked model. Taking both the Arrhenius

Table 2 V_{cmax} and J_{max} temperature response curve analysis of growth acclimated temperate and tropical trees

Model	Variable	Value at 25 °C	c	E_a or H_a	H_d	ΔS	R^2
Arrhenius function							
Tobacco grown at 25 °C	V_{cmax}^{te}	50.4	26.36	65.33	N/A	N/A	−1.56
Tobacco grown at 25 °C	V_{cmax}^{tr}	36.6	26.36	65.33	N/A	N/A	0.610
Tobacco grown at 25 °C	$V_{cmax}^{te}{}_{Radj}$	50.4	26.36	65.33	N/A	N/A	0.855
Tobacco grown at 25 °C	$V_{cmax}^{tr}{}_{Radj}$	36.6	26.36	65.33	N/A	N/A	0.953
Tobacco grown at 25 °C	$V_{cmax}^{g/25}$	1	26.36	65.33	N/A	N/A	0.968
Iteratively derived parameters	$V_{cmax}^{g/25}$	1	22.29 ± 1.4	55.01 ± 3.6	N/A	N/A	0.991
Tobacco grown at 25 °C	$J_{max}^{g/25}$	1	17.71	43.9	N/A	N/A	0.120
Peaked model							
36 species without acclimation	$V_{cmax}^{g/25}$	1	N/A	71.5	200	0.649	0.473
36 species acclimated to 35 °C	$V_{cmax}^{g/25}$	1	N/A	71.5	200	0.6309	0.965
36 species without acclimation	$J_{max}^{g/25}$	2.9	N/A	50	200	0.646	0.445
36 species acclimated to 35 °C	$J_{max}^{g/25}$	2.9	N/A	50	200	0.6335	0.744
Variable-base model							
Arrhenius function	V_{cmax}	51	22.29	55.01	N/A	N/A	0.932
Peaked model	V_{cmax}	46.8	N/A	71.5	200	Var#	0.924

The temperature response of V_{cmax} and J_{max} was modelled using either the Arrhenius function and parameters provided by Bernacchi *et al.* (2002), the peaked model with and without acclimation by Kattge & Knorr (2007) or the variable-base model proposed from this study. The scaling constant (c) and energy of activation (E_a) for the Arrhenius function, and the enthalpy (H_a), and deactivation enthalpy (H_d) in kJ mol^{-1} for the peaked function, were provided, or calculated, from the corresponding published models, except where c and E_a were estimated by iteration using a least-squares nonlinear fit (with standard error values provided) and applied to the variable-base model. The entropy term (ΔS) in kJ mol^{-1} was calculated from the slope and intercept values of linear regression analysis, provided in Kattge & Knorr (2007). V_{cmax}^{te} refers to V_{cmax} calculated for temperate species at growth temperature (T_{growth}). V_{cmax}^{tr} refers to V_{cmax} calculated for tropical species at T_{growth}. $V_{cmax}^{te}{}_{Radj}$ and $V_{cmax}^{tr}{}_{Radj}$ refer to the V_{cmax} of temperate and tropical trees with Rubisco adjusted to the content at a T_{growth} of 25 °C. $V_{cmax}^{g/25}$ of $J_{max}^{g/25}$ refers to the parameter at T_{growth} as a fraction of that measured at 25 °C. The nonlinear goodness of fit (R^2) was calculated from the combined species mean value at each temperature, and N/A refers to nonapplicable. Note that a negative R^2 means that the sum of squares for the model is greater than the sum of squares of the null hypothesis model, which is a horizontal line through the mean of all y-values.
#Indicates a variable ΔS in response to T_{growth}.

and peaked model results together, these findings suggest that acclimation to a wide range of T_{growth} values does not lead to short-term T-inhibition of V_{cmax}.

Using a similar approach as above to understand the drivers of acclimation of RuBP regeneration, we plotted J_{max} as a fraction of each species' J_{max} measured at 25 °C (J_{max}^{25}), yielding values of $J_{max}^{g/25}$ (Fig. 4b). Unlike V_{cmax}, using the T response curve of J_{max} from tobacco grown at 25 °C (Bernacchi *et al.*, 2002) did not fit the measurements of temperate and tropical trees in any meaningful way (Fig. 4b, Table 2). Using the peaked model (Kattge & Knorr, 2007) with an acclimation setting of 35 °C provided a reasonable fit (R^2 = 0.74), accounting for the diminishing increase in J_{max} at high T. However, the fit was still poor, when compared to V_{cmax} models, due to relatively high values of J_{max} in temperate trees at 15 and 20 °C.

Rubisco content implications on the long-term temperature dependence of V_{cmax}

When V_{cmax} was plotted at each prevailing T_{growth}, the long-term temperature dependence of V_{cmax} is illustrated for temperate and tropical species (Fig. 5a). Both temperate and tropical species exhibited increases in V_{cmax} with rising T_{growth}. However, when compared to the short-term temperature response function of V_{cmax} reported by Bernacchi *et al.* (2002) (shown with solid curves), this long-term V_{cmax} response to T was above expectations at 15 and 20 °C, and below expectations at 35 °C (Fig. 5a). Further, when V_{cmax} for each T_{growth} was adjusted to account for the change in Rubisco content associated with T_{growth} (Fig. 1a), the observed long-term V_{cmax} values fit the expected short-term V_{cmax} values to a much greater extent (Fig. 5b) with R^2 fits increasing from −1.56 (i.e. model fits worse than a horizontal line through the mean of V_{cmax} values) to 0.86 for temperate and 0.61 to 0.95 for tropical species (Table 2). This was evident when comparing the deviation of observed relative to expected V_{cmax}. When not adjusting for changes in Rubisco content, V_{cmax} varied by as much as 75% from that expected from the tobacco model (Fig. 5c). When changes in Rubisco were factored in, observed V_{cmax} deviated by <25% from expected model values over the entire temperature range (Fig. 5d).

The Rubisco dependent improvement in model fits of V_{cmax} plotted at each prevailing T_{growth} (Fig. 5b and d) suggests that the basal rate of V_{cmax} (i.e. V_{cmax}^{25}) acclimates to T_{growth}. Indeed, the decline in Rubisco as a % of N with increasing T_{growth} (Fig. 1e) and the associated fall in Rubisco$_a$ (Fig. 1a) led to a significant negative linear relationship between V_{cmax}^{25} and T_{growth} (Fig. 6a, Table 1). Part of the decline in V_{cmax}^{25} could be attributed to generally higher V_{cmax}^{25} values in temperate than tropical species, evident in that the V_{cmax}^{25} at T_{growth} of 25 °C was higher for temperate than tropical species. Despite the difference at 25 °C, the slope and intercept was not significantly different between biomes and a significant negative relationship was evident for the combined analysis (Table 1). As T_{growth} did not significantly influence N_a, V_{cmax}^{25} as a proportion of N ($V_{cmax}^{25}{}_{,N}$) also declined across the entire T-range (Fig. 6b). J_{max} at 25 °C (J_{max}^{25}) was lower in tropical species than their temperate counterparts, evident in a significant difference in intercept means between biomes (Fig. 6c, Table 1). Similarly, $J_{max}^{25}/V_{cmax}^{25}$ were lower in tropical than temperate species and largely independent of T_{growth}, with a significant difference in intercept means between biomes (Fig. 5d, Table 1).

Implications of changing Rubisco content on acclimation-dependent photosynthetic modelling

From the above analysis, a major factor driving acclimation of photosynthesis is T_{growth}-dependent variation in V_{cmax}^{25}, underpinned by reduced allocation of leaf N to Rubisco. Yet, T_{growth} driven changes in V_{cmax}^{25} are not factored into previously published Arrhenius and peaked temperature response functions of V_{cmax} (Eqns 5 and 6). Given this, we present a modification to the standard Arrhenius and peaked models, which factors in T_{growth}-mediated changes in V_{cmax}^{25} according to:

$$V_{cmax}^{25} = \left(86 - (1.57 * T_{growth})\right), \quad (8)$$

where the coefficient term (86 – (1.57*T_{growth})) incorporates the intercept of V_{cmax}^{25} at 0 °C (86 μmol CO_2 m^{-2} s^{-1}) and T_{growth}-dependent decline of V_{cmax}^{25} (1.57 μmol CO_2 m^{-2} s^{-1} °C^{-1}), calculated from the combined temperate and tropical linear regression analysis of V_{cmax}^{25}, as presented in Table 1. Substituting this 'variable-base' V_{cmax}^{25} coefficient term into Eqns 5 and 6 provided a good fit (R^2 = 0.93 for the Arrhenius and 0.92 for the peaked model) to the observed long-term temperature response of V_{cmax}

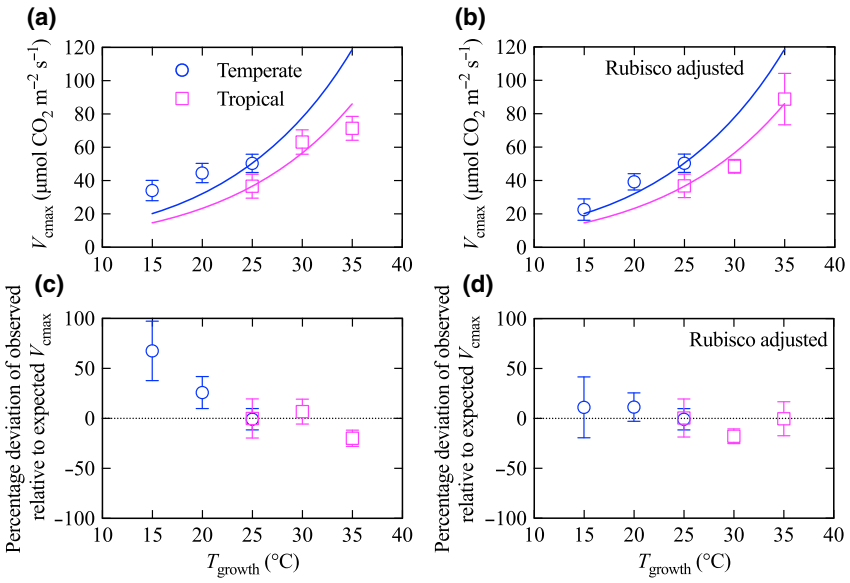

Fig. 5 The maximum CO_2 carboxylation rates (V_{cmax}), for temperate (open blue circles) and tropical (open magenta squares) trees, grown and measured from 15 to 35 °C. V_{cmax} was modelled using published Rubisco kinetic parameters of tobacco grown at 25 °C. The solid blue and magenta curves are the published tobacco temperature response function of V_{cmax}, presented by Bernacchi *et al.* (2002) and fitted to temperate and tropical species, respectively (with the T response models set to intersect measured values at 25 °C). (b) The same as Panel a but with V_{cmax} at each growth temperature adjusted to the Rubisco content measured at 25 °C [V_{cmax}/(Rubisco$_{growth}$/Rubisco$_{25\ °C}$)]. (c) The percentage deviation of observed relative to expected V_{cmax} ($V_{cmax,observed}$-$V_{cmax,expected}$/$V_{cmax,expected}$*100) at each growth temperature. (d) The same as Panel c but again with values at each growth temperature adjusted to the Rubisco content measured at 25 °C. Values are the mean ± standard error of the species means at each growth temperature.

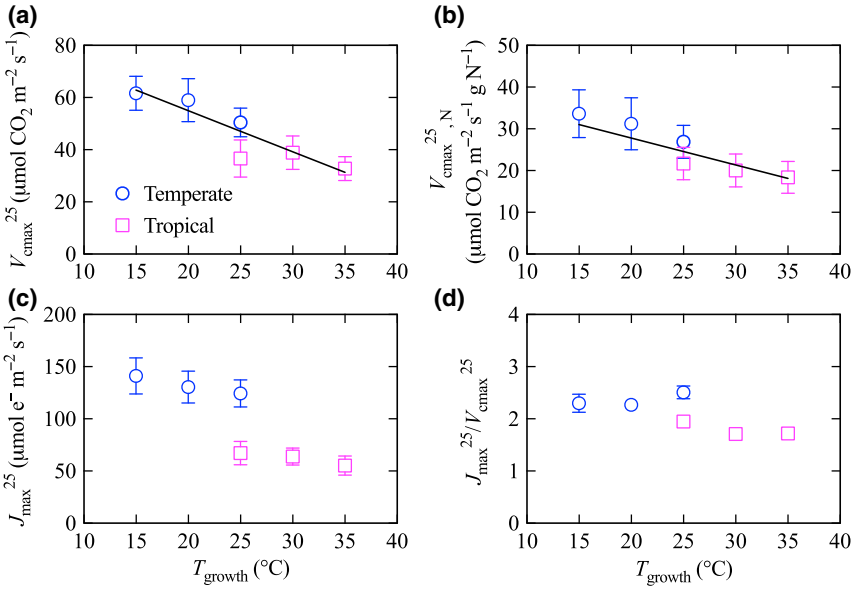

Fig. 6 The maximum CO_2 carboxylation rates (V_{cmax}) and photosynthetic electron transport rates (J_{max}) of photosynthesis for temperate (open blue circles) and tropical (open magenta squares) trees, grown from 15 to 35 °C and measured at a common temperature of 25 °C. (a) V_{cmax} measured at 25 °C (V_{cmax}^{25}). (b) V_{cmax}^{25} per unit of N on a dry mass basis ($V_{cmax,\ N}^{25}$). (c) J_{max} measured at 25 °C (J_{max}^{25}). (d) J_{max} measured at 25 °C as a fraction of V_{cmax} measured at 25 °C, ($J_{max}^{25}/V_{cmax}^{25}$). Solid black lines indicate significant ($P < 0.05$) linear regression of individual species means when temperate and tropical data sets were combined (refer to Table 1). Values are the mean ± standard error of the species means at each growth temperature.

(Fig. 7a, Table 2). The function shows a diminishing increase in V_{cmax} with T_{growth} above 25 °C and an inflection point, where V_{cmax} reaches a peak, at 40 °C.

V_{cmax} values calculated from the variable-base function (Eqn 8) of the Arrhenius and peaked model, were compared with the standard peaked function (Eqn 6), or the standard Arrhenius function (Eqn 5, with iteratively fit c and E_a values), and used to predict A_n values using Eqn 3 (Fig. 7b and c). C_c was calculated by solving Eqn 1, with A_n and C_i calculated as follows: A_n was calculated at each unit of T_{growth} from the linear regression analysis of the combined temperate and tropical species response of A_n to T_{growth} (Fig. 3a; Table 1) and C_i was fixed at a CO_2 partial pressure of 28.8 Pa (based on the assumption of a C_i/C_a of 0.75 and given that atmospheric pressure at the site of measurements averaged 96 kPa). R_{light} was fixed at the combined biome mean R_{dark} value of 1.4 μmol CO_2 m^{-2} s^{-1}, to reduce model extrapolations, considering R_{dark} was directly measured from gas-exchange and was similar in values between biomes. The resulting observed A_n values from gas-exchange and predicted A_n values using the standard V_{cmax} models (Fig, 7b), or the models with the variable-base function added (Fig. 7c), were compared (observed values as symbols; predicted values as curved fits). The standard acclimated peaked model and Arrhenius function did not fit at all closely with observed A_n (Fig. 7b). Without accounting for changes in V_{cmax}^{25}, predicted A_n was less responsive to temperature, being lower than observed values below 25 °C and higher above 25 °C. However, the variable-base model predictions (which allows for T_{growth}-dependent variations in V_{cmax}^{25}) did closely fit the observed A_n values across the entire measured T-range (Fig. 7c).

Discussion

Our study demonstrated that when a set of temperate and tropical wet-forest species experienced a range of growth temperatures similar to that experienced under field conditions, large changes in leaf structure, chemistry and function occurred. Collectively, such patterns point to common thermal acclimation responses of photosynthesis in the selected species from both biomes. Importantly, our study highlights the importance of T_{growth}-mediated changes in Rubisco abundance underpinning the acclimation response of the selected species, with the results providing an opportunity to formulate a new V_{cmax} temperature response function that accounts for acclimation-dependent changes in V_{cmax}^{25}.

Photosynthetic and respiratory adjustments to T_{growth}

We observed a linear decline in area-based concentrations of the key photosynthetic enzyme, Rubisco, with

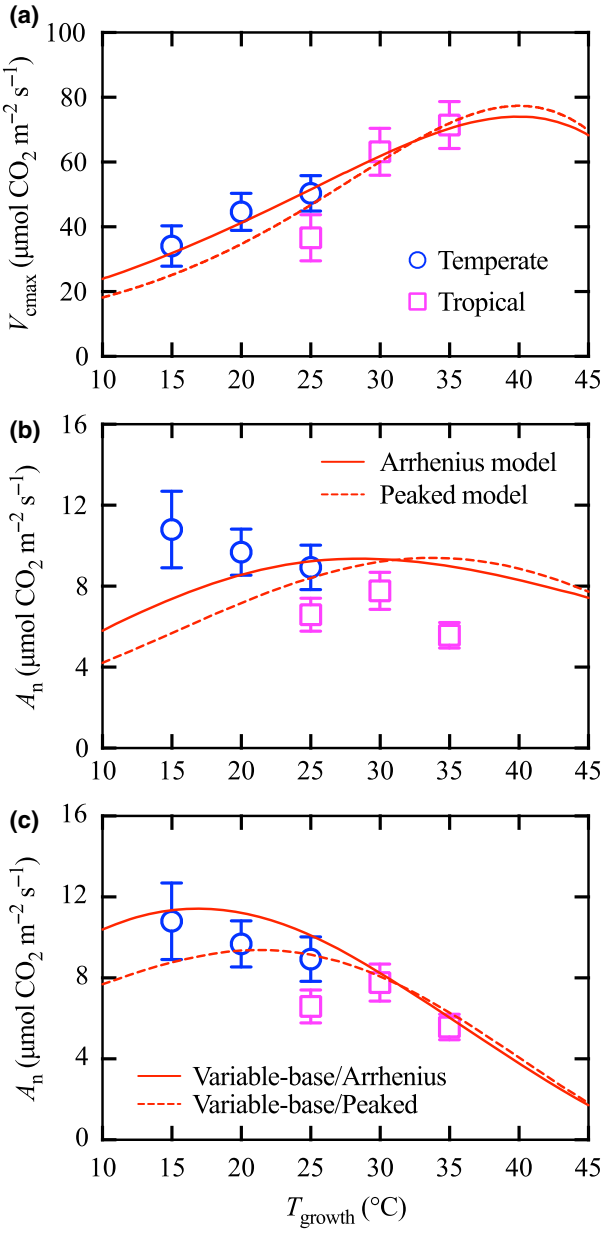

Fig. 7 The fitting of a function for predicting the acclimated response of V_{cmax} at growth temperature, and model predictions vs. observed net assimilation rates (A_n). (a) V_{cmax} measured at growth temperatures was fit with a modified Arrhenius (solid red curves) or peaked (dashed red curves) function (variable-base models), which takes into consideration the acclimation-dependent change in V_{cmax}^{25} (Eqn 8). (b) Model predictions of net photosynthesis at ambient atmospheric CO_2 (A_n), between the variable-base model (solid red curve) the acclimated peaked model of Kattge & Knorr (2007) (dashed red curve). (c) The Arrhenius and peaked models with the variable-base function (Eqn 8) incorporated. The measured net assimilation at ambient atmospheric CO_2 (A_n) of temperate (open blue circles) and tropical species (open magenta squares), the same as presented in Fig. 3, are plotted.

increasing T_{growth} (Fig. 1a, Table 1), with these changes in Rubisco content being central to the T_{growth}-dependent changes in V_{cmax}^{25} (Fig. 6) that underpin thermal acclimation responses in the selected tropical and temperate wet-forest species. From the traits measured, we see a number of factors as being responsible for the observed T_{growth}-dependent changes in Rubisco and V_{cmax}^{25}. For example, acclimation to increasing T_{growth} was associated with a decline in LMA (Fig. 1b), an observation consistent with past studies assessing T_{growth}-mediated changes in leaf structure (Poorter *et al.*, 2009). Given that LMA is influenced, in part, by leaf thickness, reduced LMA values will likely be associated with declines in the number and/or size of mesophyll cells (and thus reduced investment in photosynthetic metabolism) per unit leaf area. Yet, despite LMA decreasing with increasing T_{growth}, area-based leaf N did not decline with increasing T_{growth} (Fig. 1d), reflecting the fact that N_m exhibited a significant positive relationship with T_{growth} (Fig. 1c). While the covariance of LMA and N_m is consistent with worldwide observations of negative relationships between LMA and N_m (Reich *et al.*, 1997; Wright *et al.*, 2004), in this case it is more interesting in demonstrating that the fraction of total leaf N allocated to Rubisco (Fig. 1d) declined with increasing T_{growth} (Fig. 1e). In turn, this implies that an increasing fraction of leaf N is allocated to nonphotosynthetic components (e.g. cell wall N and/or defence compounds) as T_{growth} increases, as has been reported previously for cold and warm acclimated spinach (Yamori *et al.*, 2005). Trade-offs between leaf N investment to Rubisco vs. nonphotosynthetic components are known to occur among species differing in LMA, with high LMA species exhibiting lower relative investment of leaf N in Rubisco (Takashima *et al.*, 2004; Harrison *et al.*, 2009). Interestingly, however, these interspecific comparisons contrast with our observation that the relative N investment in Rubisco was greatest in cold grown, high LMA leaves (Fig. 1). Thus, the direction of the relationship between LMA and N investment seen in multispecies comparisons (largely driven by differences in economic strategies among species) cannot be used to predict T_{growth}-mediated changes in leaf structure and chemistry. In summary, we suggest that thermal acclimation in the temperate and tropical species is underpinned by reduced investment in photosynthetic machinery per unit leaf area that results primarily from a decline in N investment in Rubisco as T_{growth} increases.

For the declines in Rubisco and V_{cmax}^{25} at high T_{growth} to have a negative impact on assimilation rates, photosynthesis needs to be largely Rubisco-limited.

Under controlled experimental conditions of saturating light and abundant water supply, we observed A_c limitations at a C_a of 38.4 Pa, irrespective of species, biome-origin and T_{growth}, and did not observe A_r limitations until C_a values at close to 58 Pa. Of note, growth irradiance was lower than irradiance during A_n measurements; however tree species growing at low rather than high irradiance have reduced J_{max} relative to V_{cmax} (Niinemets *et al.*, 1998). This would imply that if we did grow trees at higher irradiance, matching that used for photosynthetic capacity measurements, the trees would likely remain Rubisco-limited, and to a greater extent considering J_{max} would likely limit photosynthesis at even higher CO_2 partial pressures. With the observed general A_c limitation on photosynthesis, we expected changes in Rubisco content per unit leaf area to directly impact on area-based rates of A_n and V_{cmax}. Indeed, we observed a decline in A_n with increased T_{growth} (Fig. 3, Table 1), and the long-term temperature response of V_{cmax} at T_{growth} was shallow when compared to the immediate V_{cmax} temperature response. Importantly, when Rubisco content was standardized across the T_{growth} range (i.e. ignoring any possible acclimation of Rubisco content), variation in V_{cmax} better matched the quasi-exponential T response expected by prior models (Fig. 5), which also ignore acclimation of Rubisco content, further highlighting the importance of T_{growth}-mediated changes in Rubisco in the acclimation process. Figure 8 provides a conceptual illustration, summating our generalized view of how thermal adjustments in Rubisco content impact on photosynthetic capacity.

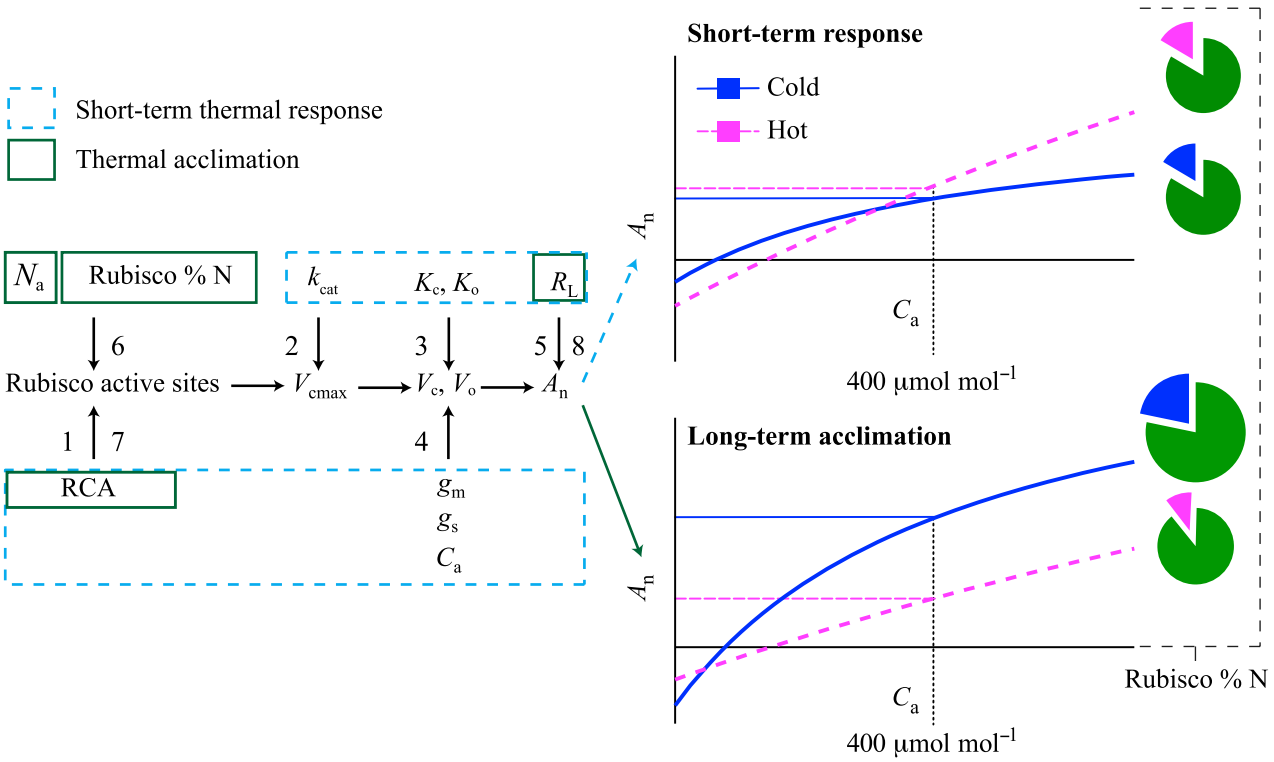

Fig. 8 A conceptual illustration of the role of Rubisco content on the short-term response and long-term thermal acclimation of net photosynthesis (A_n). The schematic diagram on the left shows the linkage between various photosynthetic carboxylation and respiration components which contribute to A_n. The immediate/short-term temperature response of A_n is dependent on: (1) changes in the number of Rubisco active sites, mediated by the Rubisco chaperone protein Rubisco activase (RCA); (2) changes in the catalytic rate constant (k_{cat}) influencing the maximum rate of carboxylation (V_{cmax}); (3) changes in Rubisco kinetic parameters (K_c and K_o) affecting the rate of carboxylation (V_c) and photorespiration (V_o); (4) CO_2 conductance from ambient air (C_a) through stomata (g_s) and mesophyll cells (g_m), affecting CO_2 substrate availability of V_c and V_o; and (5) short-term responses in light respiration (R_L). Thereafter, the long-term thermal acclimation of A_n is dependent on (6) changes in the number of Rubisco active sites, mediated by N content on a leaf area basis (N_a) and the % of N allocated to Rubisco; (7) potential adjustments in RCA thermal stability and RCA to Rubisco ratios; and (8) R_L acclimation. A generalized representation of short-term responses and long-term thermal acclimation on A_n for cold grown temperate (15 °C; blue solid lines) and hot grown tropical (35 °C; magenta dashed lines) trees are demonstrated in the right panels, with size of the pie diagrams indicating N_a and the slice representing the percentage of leaf N in Rubisco. Of note, even though Rubisco kinetic properties may not be altered, long-term thermal acclimation results in an increase in A_n for cold grown leaves and decrease in A_n for hot grown leaves at a C_a of 400 μmol mol^{-1}, driven by changes in Rubisco content.

An important consequence of the observed acclimation was that the rate of V_{cmax}^{25} at a given leaf N (i.e. photosynthetic N use efficiency) decreased with increasing T_{growth}, underpinned by the reduced allocation of leaf N to Rubisco. An earlier glasshouse comparison of 13 tropical and 12 temperate wet-forest species (Xiang *et al*., 2013), and field-based studies of tropical and temperate species (Kattge *et al*., 2009) and cool tropical/montane species (Bahar *et al*., 2016) all show lower V_{cmax}^{25} and $V_{cmax,\ N}^{25}$ in wet-forest plants growing in warmer tropical than cooler montane or temperate environments, often attributed to nutrient availability. We see, therefore, a pattern via which low V_{cmax}^{25} and $V_{cmax,\ N}^{25}$ in warm, tropical wet-forest species is likely due to the combined effects of genotypic (i.e. inherent) and environment-mediated phenotypic responses of individual plants (i.e. acclimation) to shifts in N allocation.

In past studies on thermal acclimation, growth in warm conditions resulted in greater proportional reduction in J_{max}^{25} than V_{cmax}^{25} (Atkin *et al*., 2006a; Hikosaka *et al*., 2006; Sage & Kubien, 2007; Yamori *et al*., 2010) with the result that $J_{max}^{25}/V_{cmax}^{25}$ ratios typically decreased with increasing T_{growth}. Yet, we found that $J_{max}^{25}/V_{cmax}^{25}$ was largely unresponsive to T_{growth} (Fig. 6), albeit with $J_{max}^{25}/V_{cmax}^{25}$ values being lower in the tropical than temperate trees, as was found by Xiang *et al*. (2013), evident in different intercept means. While the reasons for the lack of $J_{max}^{25}/V_{cmax}^{25}$ response to T_{growth} for the selected species remain unclear, it seems possible that J_{max}^{25} may have been overestimated in the temperate species, which were above model expectations (Fig. 4), and gave poor model fits relative to V_{cmax} (Table 2). The reason for why modelled J_{max} values did not match expectations, especially for temperate species, needs to be further explored.

We found that rates of R_{light} were always equal to or greater than R_{dark} in the temperate and tropical trees (Fig. 3e). On first inspection, this may appear a surprising result, as R_{light} is typically lower than R_{dark} – that is light inhibits leaf R (Atkin *et al*., 2006b; Zaragoza-Castells *et al*., 2007; Way & Sage, 2008; Scafaro *et al*., 2012). While there are published examples of where $R_{light} > R_{dark}$ (Atkin *et al*., 2000) – demonstrating that it is possible for respiratory fluxes to be higher in the light than in darkness – estimates of R_{light} (obtained from A_n-C_c curves) depend on the assumed Γ* value, with error in Γ* leading to concomitant errors in predicted rates of R_{light}. Given this, measurements of Γ* for both temperate and tropical trees should be a priority for future research to resolve the extent to which fluxes of R_{light} and R_{dark} differ in trees from these biomes.

Implications of short-term acclimated photosynthesis on the terrestrial biosphere

In the peaked model with acclimation considered (Kattge & Knorr, 2007), the decline in V_{cmax} at high measuring temperature is strongly influenced by the T_{growth} to which plants had acclimated, with low T_{growth} leading to reduced ΔS and a subsequent inhibition of V_{cmax} as leaves warm, even at relatively moderate temperatures (Fig. 4a). This may reflect the peaked model having being parameterized using measurements made across a range of leaf temperatures well above the T_{growth}. For example, one data set used to generate the model included several temperate tree species (*Acer pseudoplatanus*, *Betula pendula*, *Fraxinus excelsior*, *Ouercus petrea* and *Quercus robur*) grown at 16 °C and measured from 10 to 40 °C (Dreyer *et al*., 2001). We postulate that in taking measurements at temperatures far above T_{growth}, especially for cool-adapted species, inhibition of Rubisco activity is caused by a decline in the Rubisco active state. It is known that the heat-labile nature of RCA is dependent on both thermal acclimation and whether a plant is a warm- or cool-adapted species. Acclimation to warmer environments can induce thermally stable isoforms of RCA (Crafts-Brandner *et al*., 1997), and warm adapted species have evolved thermally stable RCA isoforms, relative to cool-adapted species (Salvucci & Crafts-Brandner, 2004b; Carmo-Silva & Salvucci, 2011; Scafaro *et al*., 2016). Thus, RCA inhibition would explain why V_{cmax} is predicted to decline in models generated from temperate species when measured at leaf temperatures well above T_{growth}. It would also explain why we did not see a decline in the short-term V_{cmax} temperature response for the temperate and tropical species used in our study, as we measured photosynthetic performance in leaves acclimated to each measurement T, with the growth temperatures used in our study being near that experienced by each species in their native habitat. As a result, RCA inhibition and subsequent Rubisco inactivation were unlikely in our study. In support of a lack of Rubisco inactivation, Figure S4 shows the fraction of N associated with Rubisco, calculated from observations of Rubisco from SDS-PAGE, was similar to that expected from A_c modelling (i.e. no underestimation of Rubisco by A_c modelling due to inhibited Rubisco). Consequently, we observed a short-term temperature response curve that closely matched the Arrhenius function without an inhibition term, or the peaked model with the acclimated T_{growth} set to the appropriate 35 °C, high enough to negate RCA inhibition over the measured temperature range (Fig. 4a, Table 2). This finding is in agreement with Kattge & Knorr (2007), suggesting that trees acclimated to T_{growth} within their

expected physiological range will respond to a restricted range of short-term changes in temperature *without* a V_{cmax}-driven inhibition of A_c photosynthetic capacity. Alternatively, trees experiencing extreme heating events will likely have impaired photosynthetic capacity due to a decline in V_{cmax} (Medlyn *et al*., 2002b; Kattge & Knorr, 2007). Together, these findings of stable V_{cmax} – where daily variations in leaf temperature remain relatively close to T_{growth} – and reduced V_{cmax} – where extreme heating events occur – have important implications for the modelling community as they seek to simulate plant CO_2 exchange responses to short- and long-term changes in air temperature.

Implications of thermal acclimation of photosynthesis for the terrestrial biosphere

In additional to the impact of short-term (minutes to days) shifts in measurement temperature on V_{cmax}, terrestrial biosphere models must consider longer term V_{cmax} response to temperature (Fig. 7). When considering leaves that had developed in each respective growth temperature, we found that $V_{cmax}{}^{25}$ exhibited a negative linear relationship with T_{growth} (Fig. 6). This change in the base rate of V_{cmax} will shift the Arrhenius function up or down its vertical axis, depending on long-term acclimation temperature. The variable-base model we propose accounts for this change in $V_{cmax}{}^{25}$ by incorporating the regression value for $V_{cmax}{}^{25}$ at a given T_{growth} (Eqn 8). Further refinement of the variable-base model by incorporating the temperature dependent $V_{cmax}{}^{25}$ of more temperate and tropical species should be a consideration of future work.

We made A_c model predictions using the standard Arrhenius function, the peaked model with acclimation accounted for, or both aforementioned models incorporating a variable-base function (factoring in $V_{cmax}{}^{25}$ changes), and compared the predictions with actual measurements of photosynthesis at a C_a of 38.4 Pa (Fig. 7b and c). When the variable-base function was included, both models went from poorly predicting the T response of A_n, underestimating A_n below 25 °C and overestimating above 25 °C, to being good predictors of observed A_n. This suggests that not factoring in the change in Rubisco content and subsequent change in $V_{cmax}{}^{25}$ with T_{growth} may lead to an underestimation of forest CO_2 uptake in cool climates and overestimation in warmer climates. Indeed, current models do underestimate observed forest CO_2 uptake in cooler temperate and boreal biomes and overestimate tropical biome CO_2 uptake, attributed to not factoring in differences in $V_{cmax}{}^{25}$ between PFTs (Kattge *et al*., 2009), and consistent with our findings. Of note, we observed R_{dark} and R_{light} acclimation, leading to homoeostasis of respiration in darkness and in the light across the entire 15–35 °C range. Respiratory homoeostasis reduced the amount of CO_2 lost as a proportion of photosynthetic capacity for species grown at higher temperatures, matching global observations (Atkin *et al*., 2015) and recent field-warming experiments (Aspinwall *et al*., 2016; Drake *et al*., 2016; Reich *et al*., 2016). Hence, respiratory acclimation will compensate for some of the carbon loss resulting from photosynthetic capacity downregulation and improve energy use efficiency of trees growing in a warmer world. Moreover, the demonstration from our study and the three above cited field experiments of rising respiration : photosynthesis ratios at warmer growth temperatures, despite homoeostatic or near-homoeostatic temperature acclimation of dark respiration, suggests that parameterizing respiration in models as a fixed proportion of V_{cmax} is likely inappropriate.

The reason for why there is a general trend of photosynthetic downregulation in response to T_{growth} is an intriguing question. Considering that we maintained consistent water availability and there was no significant correlation between T_{growth} and g_s, C_i or C_c, (Fig. 3c, d), we do not attribute the downregulation in photosynthesis as a response to CO_2 diffusion limitations or water stress. Reduced photosynthetic capacity in response to warmer T_{growth} may be a regulatory mechanism to balance the temperature effects on assimilate source and sink capacity (Fatichi *et al*., 2014). Similarly, plants grown under enriched ambient CO_2 alter photosynthetic capacity in response to source/sink limitations (Ainsworth *et al*., 2003; Long *et al*., 2004; Ainsworth & Long, 2005; Rosenthal *et al*., 2012).

In conclusion, the V_{cmax} temperature response of thermally acclimated trees from 15 to 35 °C displayed a standard exponential Arrhenius function, with no observable acclimation in Rubisco kinetic properties to temperature. However, the basal rate of V_{cmax} (i.e. $V_{cmax}{}^{25}$) fell with long-term acclimation to warmer T_{growth}, due to a concomitant fall in Rubisco content per unit leaf area, driven by lower N allocation to Rubisco. The result was a downward shift in photosynthesis when leaves develop in warmer environments. If these findings hold for natural ecosystems, then one might expect trees to display lower rates of photosynthesis per unit leaf area in a warmer world, regulated by a disinvestment in Rubisco.

Acknowledgements

This work was supported by the Overseas Foundation of the Chinese Academy of Sciences and National Natural Science Foundation of China (31000290, 31370594) and International Scitech Cooperation Program of China (2013DFR90670) to SX, and Australian Research Council support (FT0991448, DP0986823, DP1093759 and CE140100008 to OKA).

References

Ainsworth EA, Long SP (2005) What have we learned from 15 years of free-air CO_2 enrichment (FACE)? A meta-analytic review of the responses of photosynthesis, canopy properties and plant production to rising CO_2. *New Phytologist*, **165**, 351–372.

Ainsworth EA, Davey PA, Hymus GJ *et al.* (2003) Is stimulation of leaf photosynthesis by elevated carbon dioxide concentration maintained in the long term? A test with *Lolium perenne* grown for 10 years at two nitrogen fertilization levels under Free Air CO_2 enrichment (FACE). *Plant, Cell & Environment*, **26**, 705–714.

Ali AA, Xu C, Rogers A *et al.* (2015) Global-scale environmental control of plant photosynthetic capacity. *Ecological Applications*, **25**, 2349–2365.

Allen SE, Grimshaw HM, Parkinson JA, Quarmby C (1974) *Chemical Analysis of Ecological Materials*. Blackwell, Oxford, UK.

Arora VK, Boer GJ, Friedlingstein P *et al.* (2013) Carbon-concentration and carbon-climate feedbacks in CMIP5 earth system models. *Journal of Climate*, **26**, 5289–5314.

Aspinwall MJ, Drake JE, Campany C *et al.* (2016) Convergent acclimation of leaf photosynthesis and respiration to prevailing ambient temperatures under current and warmer climates in *Eucalyptus tereticornis*. *New Phytologist*, **212**, 354–367.

Atkin OK, Evans JR, Ball MC, Lambers H, Pons TL (2000) Leaf respiration of snow gum in the light and dark. interactions between temperature and irradiance. *Plant Physiology*, **122**, 915–923.

Atkin OK, Loveys BR, Atkinson LJ, Pons TL (2006a) Phenotypic plasticity and growth temperature: understanding interspecific variability. *Journal of Experimental Botany*, **57**, 267–281.

Atkin OK, Scheurwater I, Pons TL (2006b) High thermal acclimation potential of both photosynthesis and respiration in two lowland *Plantago* species in contrast to an alpine congeneric. *Global Change Biology*, **12**, 500–515.

Atkin OK, Bloomfield KJ, Reich PB *et al.* (2015) Global variability in leaf respiration in relation to climate, plant functional types and leaf traits. *New Phytologist*, **206**, 614–636.

Badger MR, Björkman O, Armond PA (1982) An analysis of photosynthetic response and adaptation to temperature in higher plants: temperature acclimation in the desert evergreen *Nerium oleander* L*. *Plant, Cell & Environment*, **5**, 85–99.

Bahar NHA, Ishida FY, Weerasinghe LK *et al.* (2016) Leaf-level photosynthetic capacity in lowland Amazonian and high-elevation, Andean tropical moist forests of Peru. *New Phytologist*, doi: 10.1111/nph.14079.

Beer C, Reichstein M, Tomelleri E *et al.* (2010) Terrestrial gross carbon dioxide uptake: global distribution and covariation with climate. *Science*, **329**, 834–838.

Bernacchi CJ, Portis AR, Nakano H, von Caemmerer S, Long SP (2002) Temperature response of mesophyll conductance. Implications for the determination of rubisco enzyme kinetics and for limitations to photosynthesis *in vivo*. *Plant Physiology*, **130**, 1992–1998.

Berry J, Bjorkman O (1980) Photosynthetic response and adaptation to temperature in higher plants. *Annual Review of Plant Physiology*, **31**, 491–543.

Bruhn D, Mikkelsen TN, Atkin OK (2002) Does the direct effect of atmospheric CO_2 concentration on leaf respiration vary with temperature? Responses in two species of *Plantago* that differ in relative growth rate. *Physiologia Plantarum*, **114**, 57–64.

von Caemmerer S (2000) *Biochemical Models of Leaf Photosynthesis*. CSIRO Publishing, Collingwood, Vic.

von Caemmerer S, Evans JR (2015) Temperature responses of mesophyll conductance differ greatly between species. *Plant, Cell & Environment*, **38**, 629–637.

Canadell JG, Le Quéré C, Raupach MR *et al.* (2007) Contributions to accelerating atmospheric CO_2 growth from economic activity, carbon intensity, and efficiency of natural sinks. *Proceedings of the National Academy of Sciences of the United States of America*, **104**, 18866–18870.

Carmo-Silva E, Salvucci M (2011) The activity of Rubisco's molecular chaperone, Rubisco activase, in leaf extracts. *Photosynthesis Research*, **108**, 143–155.

Cheesman AW, Winter K (2013) Growth response and acclimation of CO_2 exchange characteristics to elevated temperatures in tropical tree seedlings. *Journal of Experimental Botany*, **64**, 3817–3828.

Crafts-Brandner SJ, Salvucci ME (2000) Rubisco activase constrains the photosynthetic potential of leaves at high temperature and CO_2. *Proceedings of the National Academy of Sciences of the United States of America*, **97**, 13430–13435.

Crafts-Brandner SJ, van de Loo FJ, Salvucci ME (1997) The two forms of ribulose-1,5-bisphosphate carboxylase/oxygenase activase differ in sensitivity to elevated temperature. *Plant Physiology*, **114**, 439–444.

Cunningham SC, Read JR (2002) Comparison of temperate and tropical rainforest tree species: photosynthetic responses to growth temperature. *Oecologia*, **133**, 112–119.

Cunningham SC, Read J (2003) Do temperate rainforest trees have a greater ability to acclimate to changing temperatures than tropical rainforest trees? *New Phytologist*, **157**, 55–64.

Drake JE, Tjoelker MG, Aspinwall MJ, Reich PB, Barton CVM, Medlyn BE, Duursma RA (2016) Does physiological acclimation to climate warming stabilize the ratio of canopy respiration to photosynthesis? *New Phytologist*, **211**, 850–863.

Dreyer E, Le Roux X, Montpied P, Daudet FA, Masson F (2001) Temperature response of leaf photosynthetic capacity in seedlings from seven temperate tree species. *Tree Physiology*, **21**, 223–232.

Dufresne J-L, Foujols M-A, Denvil S *et al.* (2013) Climate change projections using the IPSL-CM5 Earth System Model: from CMIP3 to CMIP5. *Climate Dynamics*, **40**, 2123–2165.

Ellsworth DS, Crous KY, Lambers H, Cooke J (2015) Phosphorus recycling in photorespiration maintains high photosynthetic capacity in woody species. *Plant, Cell & Environment*, **38**, 1142–1156.

Farquhar GD, von Caemmerer S, Berry JA (1980) A biochemical model of photosynthetic CO_2 assimilation in leaves of C_3 species. *Planta*, **149**, 78–90.

Fatichi S, Leuzinger S, Körner C (2014) Moving beyond photosynthesis: from carbon source to sink-driven vegetation modeling. *New Phytologist*, **201**, 1086–1095.

Gaspar MM, Ferreira RB, Chaves MM, Teixeira AR (1997) Improved method for the extraction of proteins from Eucalyptus leaves. Application in leaf response to temperature. *Phytochemical Analysis*, **8**, 279–285.

Harrison MT, Edwards EJ, Farquhar GD, Nicotra AB, Evans JR (2009) Nitrogen in cell walls of sclerophyllous leaves accounts for little of the variation in photosynthetic nitrogen-use efficiency. *Plant, Cell & Environment*, **32**, 259–270.

Hikosaka K (1997) Modelling optimal temperature acclimation of the photosynthetic apparatus in C3 plants with respect to nitrogen use. *Annals of Botany*, **80**, 721–730.

Hikosaka K, Murakami A, Hirose T (1999) Balancing carboxylation and regeneration of ribulose-1,5-bisphosphate in leaf photosynthesis: temperature acclimation of an evergreen tree, *Quercus myrsinaefolia*. *Plant, Cell & Environment*, **22**, 841–849.

Hikosaka K, Ishikawa K, Borjigidai A, Muller O, Onoda Y (2006) Temperature acclimation of photosynthesis: mechanisms involved in the changes in temperature dependence of photosynthetic rate. *Journal of Experimental Botany*, **57**, 291–302.

Kattge J, Knorr W (2007) Temperature acclimation in a biochemical model of photosynthesis: a reanalysis of data from 36 species. *Plant, Cell & Environment*, **30**, 1176–1190.

Kattge J, Knorr W, Raddatz T, Wirth C (2009) Quantifying photosynthetic capacity and its relationship to leaf nitrogen content for global-scale terrestrial biosphere models. *Global Change Biology*, **15**, 976–991.

Kromdijk J, Long SP (2016) One crop breeding cycle from starvation? How engineering crop photosynthesis for rising CO_2 and temperature could be one important route to alleviation. *Proceedings of the Royal Society of London B: Biological Sciences*, **283**, doi: 10.1098/rspb.2015.2578.

Lambers H, Chapin FS, Pons TL (1998) Photosynthesis, respiration, and long-distance transport. In: *Plant Physiological Ecology* (eds Lambers H, Chapin FS, Pons TL), pp. 10–153. Springer New York, New York, NY.

Long SP, Ainsworth EA, Rogers A, Ort DR (2004) Rising atmospheric carbon dioxide: plants FACE the future. *Annual Review of Plant Biology*, **55**, 591–628.

Medlyn BE, Dreyer E, Ellsworth D *et al.* (2002a) Temperature response of parameters of a biochemically based model of photosynthesis. II. A review of experimental data. *Plant, Cell & Environment*, **25**, 1167–1179.

Medlyn BE, Loustau D, Delzon S (2002b) Temperature response of parameters of a biochemically based model of photosynthesis. I. Seasonal changes in mature maritime pine (*Pinus pinaster Ait.*). *Plant, Cell & Environment*, **25**, 1155–1165.

Niinemets Ü, Kull O, Tenhunen JD (1998) An analysis of light effects on foliar morphology, physiology, and light interception in temperate deciduous woody species of contrasting shade tolerance. *Tree Physiology*, **18**, 681–696.

Onoda Y, Hikosaka K, Hirose T (2005) Seasonal change in the balance between capacities of RuBP carboxylation and RuBP regeneration affects CO_2 response of photosynthesis in *Polygonum cuspidatum*. *Journal of Experimental Botany*, **56**, 755–763.

Pan Y, Birdsey RA, Fang J *et al.* (2011) A large and persistent carbon sink in the world's forests. *Science*, **333**, 988–993.

Poorter H, Niinemets Ü, Poorter L, Wright IJ, Villar R (2009) Causes and consequences of variation in leaf mass per area (LMA): a meta-analysis. *New Phytologist*, **182**, 565–588.

Portis A (2003) Rubisco activase – rubisco's catalytic chaperone. *Photosynthesis Research*, **75**, 11–27.

Reich PB, Walters MB, Ellsworth DS (1997) From tropics to tundra: global convergence in plant functioning. *Proceedings of the National Academy of Sciences of the United States of America*, **94**, 13730–13734.

Reich PB, Sendall KM, Stefanski A, Wei X, Rich RL, Montgomery RA (2016) Boreal and temperate trees show strong acclimation of respiration to warming. *Nature*, **531**, 633–636.

Rogers A (2013) The use and misuse of Vc, max in Earth System Models. *Photosynthesis Research*, **119**, 15–29.

Rosenthal DM, Slattery RA, Miller RE *et al.* (2012) Cassava about-FACE: greater than expected yield stimulation of cassava (*Manihot esculenta*) by future CO_2 levels. *Global Change Biology*, **18**, 2661–2675.

Ruuska S, Andrews TJ, Badger MR, Hudson GS, Laisk A, Price GD, von Caemmerer S (1998) The interplay between limiting processes in C_3 photosynthesis studied by rapid-response gas exchange using transgenic tobacco impaired in photosynthesis. *Functional Plant Biology*, **25**, 859–870.

Sage RF (2002) Variation in the kcat of Rubisco in C_3 and C_4 plants and some implications for photosynthetic performance at high and low temperature. *Journal of Experimental Botany*, **53**, 609–620.

Sage RF, Kubien DS (2007) The temperature response of C_3 and C_4 photosynthesis. *Plant, Cell & Environment*, **30**, 1086–1106.

Sage RF, Way DA, Kubien DS (2008) Rubisco, Rubisco activase, and global climate change. *Journal of Experimental Botany*, **59**, 1581–1595.

Salvucci ME, Crafts-Brandner SJ (2004a) Inhibition of photosynthesis by heat stress: the activation state of Rubisco as a limiting factor in photosynthesis. *Physiologia Plantarum*, **120**, 179–186.

Salvucci ME, Crafts-Brandner SJ (2004b) Relationship between the heat tolerance of photosynthesis and the thermal stability of rubisco activase in plants from contrasting thermal environments. *Plant Physiology*, **134**, 1460–1470.

Scafaro AP, Yamori W, Carmo-Silva AE, Salvucci ME, von Caemmerer S, Atwell BJ (2012) Rubisco activity is associated with photosynthetic thermotolerance in a wild rice (*Oryza meridionalis*). *Physiologia Plantarum*, **146**, 99–109.

Scafaro AP, Gallé A, Van Rie J, Carmo-Silva E, Salvucci ME, Atwell BJ (2016) Heat tolerance in a wild Oryza species is attributed to maintenance of Rubisco activation by a thermally stable Rubisco activase ortholog. *New Phytologist*, **211**, 899–911.

Sharkey TD (1985) O_2-Insensitive photosynthesis in C_3 plants: its occurrence and a possible explanation. *Plant Physiology*, **78**, 71–75.

Sharkey TD, Bernacchi CJ, Farquhar GD, Singsaas EL (2007) Fitting photosynthetic carbon dioxide response curves for C_3 leaves. *Plant, Cell and Environment*, **30**, 1035–1040.

Smith NG, Dukes JS (2013) Plant respiration and photosynthesis in global-scale models: incorporating acclimation to temperature and CO_2. *Global Change Biology*, **19**, 45–63.

Takashima T, Hikosaka K, Hirose T (2004) Photosynthesis or persistence: nitrogen allocation in leaves of evergreen and deciduous *Quercus* species. *Plant, Cell & Environment*, **27**, 1047–1054.

Way DA, Oren R (2010) Differential responses to changes in growth temperature between trees from different functional groups and biomes: a review and synthesis of data. *Tree Physiology*, **30**, 669–688.

Way DA, Sage RF (2008) Thermal acclimation of photosynthesis in black spruce [*Picea mariana* (Mill.) B.S.P.]. *Plant, Cell & Environment*, **31**, 1250–1262.

Way D, Yamori W (2014) Thermal acclimation of photosynthesis: on the importance of adjusting our definitions and accounting for thermal acclimation of respiration. *Photosynthesis Research*, **119**, 89–100.

Wright IJ, Reich PB, Westoby M *et al.* (2004) The worldwide leaf economics spectrum. *Nature*, **428**, 821–827.

Xiang S, Reich PB, Sun S, Atkin OK (2013) Contrasting leaf trait scaling relationships in tropical and temperate wet forest species. *Functional Ecology*, **27**, 522–534.

Yamori W, Noguchi K, Terashima I (2005) Temperature acclimation of photosynthesis in spinach leaves: analyses of photosynthetic components and temperature dependencies of photosynthetic partial reactions. *Plant, Cell & Environment*, **28**, 536–547.

Yamori W, Suzuki K, Noguchi KO, Nakai M, Terashima I (2006) Effects of Rubisco kinetics and Rubisco activation state on the temperature dependence of the photosynthetic rate in spinach leaves from contrasting growth temperatures. *Plant, Cell & Environment*, **29**, 1659–1670.

Yamori W, Noguchi K, Hikosaka K, Terashima I (2010) Phenotypic plasticity in photosynthetic temperature acclimation among crop species with different cold tolerances. *Plant Physiology*, **152**, 388–399.

Zaragoza-Castells J, Sánchez-Gómez D, Valladares F, Hurry V, Atkin OK (2007) Does growth irradiance affect temperature dependence and thermal acclimation of leaf respiration? Insights from a Mediterranean tree with long-lived leaves. *Plant, Cell & Environment*, **30**, 820–833.

Supporting Information

Additional Supporting Information may be found in the online version of this article:

Figure S1. Representative SDS-PAGE gel, used for determining leaf Rubisco content.
Figure S2. Individual species plots of Rubisco content and $V_{cmax}{}^{25}$ versus T_{growth}.
Figure S3. Representative A_n-C_c curves, for all 10 species, at each measurement temperature.
Figure. S4. A comparison of Rubisco as a fraction of N, calculated from protein assays or A_c-modelling.
Table S1 Ecological niche, provenance, and sourcing details of the species used in this study.
Table S2. Leaf trait values for each temperate tree species at growth temperatures of 15, 20 and 25 °C.
Table S3. Leaf trait values for each tropical tree species at growth temperatures of 25, 30 and 3